

## ABSTRACT

Title of Document: FIRE GROWTH EVALUATION FOR REGULATIONS OF FIRE LOAD FOR TYPE 5A SPACES ON SEAFARING VESSELS.

Noel Thomas Shriner, Fire Protection Engineering, 2012

Directed By: Assistant Professor, Ph.D., Stanislav I. Stoliarov, Department of Fire Protection Engineering

An evaluation of the current materials in class 5A spaces was conducted to ensure the fire load specified in US Coast Guard regulation 46 CFR subchapter K of 5 kg/m<sup>2</sup> does not cause life endangerment. Cone calorimeter testing of seat foam and fabric determined time to ignition dependant on heat flux. Total heat release rate was calculated through full scale testing of seats common in class 5A spaces. A Fire Dynamic Simulator (FDS) model of a class 5A space with data from previous tests was then used to calculate heat transfer into ceiling to determine if flashover occurs and if the exposed upper deck surface temperature reaches a critical 232° C value when passenger safety is jeopardized due to structural integrity loss of aluminum. Theoretical calculations verified FDS thermal and physical properties with temperatures remaining at a level below the critical value.

FIRE GROWTH EVALUATION FOR REGULATIONS OF FIRE LOAD FOR  
TYPE 5A SPACES ON SEAFARING VESSELS

By

Noel Thomas Shriner

Thesis submitted to the Faculty of the Graduate School of the  
University of Maryland, College Park, in partial fulfillment  
of the requirements for the degree of  
Master of Science  
2012

Advisory Committee:  
Professor Stanislav I. Stoliarov, Chair  
Professor Arnaud C. Trouvé  
Professor Peter B. Sunderland

© Copyright by  
Noel Thomas Shiner  
2012

## Acknowledgements

The testing for this report would not have been possible without the help of many people. People from the University of Maryland and the US Coast Guard came together to make this possible. I would first like to thank Professor Stanislav I. Stoliarov for being my advisor and guiding me throughout. His guidance and knowledge has enabled this testing to be as accurate as possible with the resources provided. I would also like to thank Olga Zeller for her help with testing in the burn lab and cone calorimeter. Tom Woodford of the Marine Safety Center USCG provided me with this topic and aided as a liaison helping obtain samples and documentation for testing. The samples of foam fabric and seats came from the donation of Gladding-Hearn Shipbuilding. Without their help with providing these materials and shipping them quickly, testing would have not have been possible.

# Table of Contents

Acknowledgements.....	ii
Table of Contents.....	iii
List of Tables.....	v
List of Figures.....	v
Chapter 1: Introduction.....	1
Approach.....	4
Chapter 2: Fire Load.....	7
Determining Components in the Fire Load.....	7
Chapter 3: Time to Ignition.....	12
Theory of Ignition.....	12
Ignition Testing.....	13
Sample.....	13
Cone Calorimetry Testing.....	14
Chapter 4: Heat of Combustion.....	17
Cone Calorimeter $\Delta H_c$ Testing.....	17
Sample Heat of Combustion.....	18
Chapter 5: Heat Release Rate.....	19
Testing Setup.....	19
Setup.....	20
Testing Results.....	23
Mass Loss Rate.....	23
Heat Release Rate.....	25
FDS HRR Curves.....	26
Chapter 6: FDS Radiative Fraction Adjustment.....	29
FDS Model.....	29
Burn Lab Model.....	29
Chair Model.....	31

Results.....	32
Chapter 7: FDS Full Scale Simulation.....	35
Full Scale FDS model.....	35
5A Space.....	35
Virtual Measurement Points.....	36
Full Scale Simulation.....	39
Seat Orientations Tested.....	39
Determining Ignition Times.....	41
Deck Temperature.....	45
Chapter 8: FDS Model Adjustments and Corrections.....	47
Mesh Size Adjustments.....	47
Conduction.....	51
Convection.....	51
Radiation.....	60
Conclusion.....	65
Appendix A: Small Scale FDS vs. Full Scale Chair Testing.....	67
Appendix B: FDS Full Scale Testing.....	72
Bibliography.....	77

## List of Tables

Table 1: Adjacent HFG orientation and distance for each test. Asterisk denotes no ignition. ....	22
Table 2: Fitted curve numerical values set to start burning at time zero. The area under the curve was then measured against the total heat released from full scale testing to ensure these values matched. ....	29
Table 3: Fire Loads simulated in FDS. Areas vary with how the rows are configured with each other. ....	40

## List of Figures

Figure 1: Ocean Contour 200 seat which specific foam components. ....	9
Figure 2: Foam and fabric sample easily ignited with a light and able to sustain a flame. ....	10
Figure 3: Flame spread test on carpet using 50 mL of heptane fuel. Only the heptane burned on the surface of the carpet. ....	11
Figure 4: Cone samples of the carpet after exposure to 15, 20, and 25 kW/m <sup>2</sup> heat flux in the cone calorimeter. Background carpet was not tested. ....	12
Figure 5: Cone calorimeter sample before testing ....	14
Figure 6: Time for the sample to ignite to a respective heat flux. Critical heat flux line represents the lowest heat flux value the sample would ignite at. ....	15
Figure 7: $1/t_{ig}^{-1/2}$ versus heat flux. Having a more linear representation allows for an increase in accuracy calculating the time to ignition. As heat flux reaches to a critical temperature, this linearity breaks down causing a curve. ....	16
Figure 8: Incomplete burn of a sample tested at 20 kW/m <sup>2</sup> (left) and complete burn at 50 kW/m <sup>2</sup> (right) ....	17
Figure 9: Graph of heat of combustion for seat samples in cone calorimeter tests. Far right bar represents average of all samples tested. ....	19
Figure 10: Seat assembly for full scale testing. ....	21

Figure 11: Mass data obtain from the scale. Tests 2-4 represent seats with a middle ignition and tests 7 and 8 a side ignition source. ....	23
Figure 12: Sample chair fully engulfed (left) and a chair after extinguished (right)..	24
Figure 13: Average mass loss rate for middle and side ignitions. Middle ignition burned quicker due to faster flame spread across the seat. ....	25
Figure 14: HRR calculated from MLR and $\Delta H_c$ . The HRR is proportional to how quickly the flames spread across the chair, making a middle ignition burn quicker but have the same total heat released since all chairs had similar fuel loads.....	26
Figure 15: Fitted curve for middle ignition. 1.9% error. ....	28
Figure 16: Fitted curve for side ignition. 0.1% error .....	28
Figure 17: Small scale FDS model to simulate the burn lab used in full scale testing. ....	32
Figure 18: Heat flux data obtains at the back rest of the chair, 7.5 cm away. Ignition source in middle of chair.....	33
Figure 19: Heat flux data representing the next row of seats fwd of the burning chair. Ignition source on side of chair.....	33
Figure 20: Heat flux data obtained near the seat bottom cushion 22.5 cm away. Heat flux gauges were tilted 45 degrees towards the burn chair. Ignition at side of chair..	34
Figure 21: Model of the 5A space used for testing with labeling and space dimensions. Some rows were taken out to reduce clutter for illustration.....	36
Figure 22: Profile of the temperature gradient of the air within the space. The fire plume coming from the chairs is distinctly higher than the ambient temperature in the rest of the space.....	38
Figure 23: Temperature gradient of the outer walls of the space. Higher temperatures are centered around where the fire plume's impingement region contacts the wall...	38
Figure 24: Smoke layer forming at the upper boundary of the space as the seats burn. ....	39
Figure 25: Fire Load area depending on row orientations. Rows with chairs aligned the same way only require 1 row in area for the module. The box provides area for the seats and aisle room. ....	39

Figure 26: Average heat flux over time. These two values will be compared to what was determine through cone testing. HF Ave 14.5 kW/m <sup>2</sup> over 130 seconds.....	41
Figure 27: Time to ignition calculation comparing FDS heat flux to the time to ignition curve from cone testing. FDS time is above ignition time for 14.5 kW/m <sup>2</sup> , therefore the seat will ignite at 275 seconds. ....	42
Figure 28: Total heat released by two chairs burning at the same rate. This rate simulates a chair with an ignition source at the middle of the seat. As more heat is released the adjacent chairs ignite.....	44
Figure 29: Total heat released by six chairs burning. The adjacent chairs ignited have the side ingition HRR curve since ignited by adjacent seats. ....	44
Figure 30: Total HRR with chair ignition points (black lines) and amount of chairs burning. ....	45
Figure 31: Visual of fire spread across the 10 chairs. No other seats in other aisles or rows ignited since heat flux was below the critical value.....	45
Figure 32: Upper deck temperatures from FDS testing. ....	46
Figure 33: Convective heat flux comparison of mesh sizes. ....	49
Figure 34: Radiative heat flux comparison of mesh sizes. ....	50
Figure 35: Temperature difference between mesh resolutions.....	50
Figure 36: FDS vs theoretical values of convective heat flux at the ceiling.....	54
Figure 37: FDS vs theoretical values with convective correction. ....	55
Figure 38: FDS with convection correction vs Alpert's for 5 by 5 seat orientation. ..	56
Figure 39: Impingement region fire plume temperature. ....	59
Figure 40: Temperature comparison of the old and new convective coefficients. ....	60
Figure 41: Picture of the smoke layer used to determine temperature and absorption coefficient. ....	62
Figure 42: Average smoke layer temperature over a 1 meter span.....	63
Figure 43: Smoke layer re-radiation value.....	64
Figure 44: Final upper deck temperatures with all corrections completed. ....	65

## Chapter 1: Introduction

Fire is a big concern with any type of structure, but none more important than on a sea going vessel. When a ship catches fire out at sea, there is no fire department to help and only the people on board can save themselves. This is one of the main reasons why vessel regulations dealing with fire protection are more stringent than their land counterparts. Fire protection depends on many variables and characteristics of the vessel. The size and its cargo are what determine its classification and types of fire protection it requires in order to be considered safe at sea. From this general classification come more specific regulations dealing with the type of spaces found on board.

One space in particular when dealing with passenger vessels only requires a minimal amount of fire protection. This space is categorized as a very low fire load space, or commonly called type 5A space. The policies regarding these types of spaces are intended to provide a consistent level of fire protection, while permitting weight savings which directly affects fuel efficiency, capacity and stability [1]. These spaces are only permitted on passenger vessels carrying 600 or less people and do not have any overnight accommodations. Class 5A space commonly found on high speed ferries or tourist excursion vessels. The fire load value is enforced by 46 CFR Subchapter K and guidance is provided through the Navigation and Vessel Inspection Circular (NVIC) 9-97.

Although there are many regulations [1] that apply for a space being characterized as a 5A space, the main restriction is the total allowable fuel load. A type 5A space must have a uniform combustible load of less than  $5 \text{ kg/m}^2$  which includes  $0.75 \text{ kg/m}^2$  for

passenger effects. This fire load value accounts for the entire fire load for the space. This is easily calculated by taking the total fire load within the space and dividing it by the total area. As long as it is below  $5 \text{ kg/m}^2$  the space can be categorized as 5A. In order to simplify these calculations, the fire load is considered a universal unit to all flammable materials and only accounts for the weight and no other thermal properties.

The concern that initiated this evaluation is the fire load may be too high and could cause localized temperatures within the space to reach a value where structural integrity becomes an issue. Manufacturers are using lighter and cheaper materials in order to reduce weight with minimal concern with its thermal properties. All materials do not burn at the same rate or intensity, so imposing a general weight restriction could actually cause a fire to burn hotter and longer depending on the material which could lead to structural failure.

A test in the mid 90's was conducted by the Coast Guard to evaluate flashover possibilities in type 5A spaces [3]. Flashover is defined as a point when all combustible materials in an enclosed area are heated to their auto ignition temperature and release combustible vapors. In these experiments, fuel load density, material fire resistance, and fuel package distribution was tested in a space to determine if flashover could occur. The test was completed in a steel compartment with nominal dimensions of 4.6 m wide, by 5.0 m deep by 2.5 m high. They tested a variety of combustible classified seats in a variety of fuel load values in order to see if this could cause a space flashover. The results from this experiment showed that flashover does not occur even when they burned a stack of 36 seat cushions in the center of the

space. It did show, though, that fuel load density, fuel load material properties, and fuel load package distribution will each impact the severity of the fire [3].

These full scale experiments showed that flashover did not occur with the restricted fuel load. These experiments emphasis was on flashover possibilities of type 5A spaces and not structural integrity. Typically 5A spaces are constructed out of aluminum instead of steel in order to save weight. The previous experiments were conducted in a small steel space and STAR\*CD, a computational fluid dynamics program (CFD), was used to extrapolate the data to make the space act like it was made out of aluminum [3]. This was conducted back in 1997 and CFD programs today have become more refined and accurate with computational power tremendously more powerful.

The goal for this testing was to build on what was previously completed with full scale testing and accurately measure the temperature in the space using a mixture of full scale testing and CFD program. Temperature is the biggest concern since the aluminum structure is considered to start losing structural rigidity at 232°C and beings to melt in the range of 500°C to 670°C [1]. Due to the immense size of 5A spaces, the area of refuge in case of an emergency is above. With the added weight of passengers on the upper deck, the structural integrity of the aluminum space is even more important to provide safety. This is why the 232° C is considered a critical temperature since it is when the possibility of structural failure can occur.

The other concern for passenger safety with fires is the time required to abandon the ship. The current regulation for passenger stay time in an area of refuge is either the time required completing disembarking of the vessel or one hour, whichever is less

[4]. The time used for this testing is the one hour mark since it is desired to determine the maximum temperature at the longest time a passenger would be on the vessel.

Using a hybrid of devices and computer programs to increase accuracy of testing, the 5 kg/m<sup>2</sup> fire load for class 5A spaces will be evaluated to determine if the upper deck reaches the critical temperature of 232 °C within the one hour stay time of passengers in the area of refuge.

### Approach

There are many types of resources that can be used to study the combustion reaction. Each can test for a specific aspect and can be very accurate. The problem with this experiment is that it incorporates many variables dealing with combustion and fire growth in which no single method can depict, and because of this, an array of testing methods was needed to come up with accurate results. Testing was completed using different types of full scale and computational simulations to provide the most accurate data needed.

First was to determine what in the space is considered a part of the fuel load. Seat foam and fabric as well as the carpet typically found in class 5A spaces are determined to possibly provide the most amounts to the fire load. A couple simple tests were conducted to verify that these materials do ignite and sustain a flame. The first test attempted was to see if it would ignite using a simple hand grill lighter. If the material was able to hold combustion additional testing was then completed to determine specific properties for use in FDS to simulate the burning of these materials. If the material does not ignite and sustain a flame, then no further testing was required since it will not contribute to the fire load.

Cone calorimeter testing was then used to help determine the ignition curves of the materials that were considered part of the fuel load. The cone can determine the time to ignition by exposing the material to a fixed heat flux and observing when it ignites. Varying this heat flux will change the ignition time and is used to generate an ignition curve.

The cone can also determine the heat of combustion of a material by measuring the heat release rate and mass loss rate. Mass loss rate is gathered using a scale that the material is tested on. Heat release rate was determined by the cone used through the oxygen consumption method [5].

Full scale chair testing was used to determine the mass loss rate during combustion. Heat released from a combustible material is a product of the total mass consumed during combustion and the heat of combustion of the material. The cone was already used for heat of combustion so determining the rate of mass consumed is calculated by burning the material on a scale. This approach provides a very accurate curve that characterizes how the seat will burn if ignited under typical conditions.

The use of a CFD program to model fire growth and spread is a more practical solution than doing full scale tests. An accurate model was created which can simulate what can occur in real life using the heat release rate and time to ignition curves determined earlier. There are many commercial CFD programs available for simulations but only a few have been tailored for fire dynamics. One is the Fire Dynamics Simulator (FDS).

FDS was created by the National Institute of Standards and Technology (NIST) in 2000 to aid in fire modeling [7]. FDS solves numerically a form of the Navier-Stokes equations for low-speed, thermally-driven flows with emphasis on smoke and heat transport from fires [8]. The input parameters required by FDS to describe a certain situation are conveyed using a single text file generated by the user. This text file represents all the parameters needed to build and test the model to the users discretion.

Although FDS is a powerful modeling program, it still has its limitations with accurately depicting the volatilization and combustion of specific materials. The most complex parameters in FDS are set to a default value that the developers consider to be a general value for standard models. These values can be altered by the user to make FDS predict results closer to what is seen for the situation.

A model of a type 5A space was constructed typical to the dimensions seen on vessels constructed. To simplify the FDS model, the chairs are represented by burners with a fixed heat release rate. By simplifying the model, it is more controllable as to how it will react and thus easier to match real testing done. The problem with simplifying it this much is that FDS will not determine when adjacent materials will ignite from an outside heat source. FDS uses thermal and physical properties of materials to determine when the material reaches a temperature where volatile fumes are released and can ignite. None of these properties are used in this experiment since they were not readily available and because of the complexity of the material on the seats.

Determining ignition times for the seats was calculated by taking the average heat flux the adjacent seats were exposed to and comparing this value to the ignition time

curves. The time at which the seat ignites was when it was exposed long enough at that heat flux to allow ignition.

A variety of orientations and fuel loads were tested in the modeled space to determine if structural integrity was ever jeopardized. The seats were oriented in different rows and ways they were facing. The rows reached a maximum of 5 seats each since this is typically the maximum number seen before an aisle separates the next section. This also reduces the overall fire load for the space to be in compliance. In all, a variety of seat orientations and number were tested reaching a maximum of 10 seats with a maximum fuel load of  $5.0 \text{ kg/m}^2$ .

The thermal properties in FDS were also adjusted to ensure the model portrayed every possible scenario that could possibly happen. Testing the highest possible situation of radiative and convective heat transfer appropriate to the fire produced by the chairs makes certain that all variables were tested. With no other outcome possible, the final results of the testing can be used to justify whether the regulation in place now is sufficient or not.

## Chapter 2: Fire Load

### *Determining Components in the Fire Load*

The amount of fire load within a class 5A space is limited to  $5 \text{ kg/m}^2$  as regulated under NVIC 9-97 [1]. This value takes in to account all materials that are considered combustible. The most common materials within class 5A spaces were taken into account and tested to see if they do ignite and account towards the regulated fire load.

Seats

The seats contain a heterogeneous mixture of foam and fabric outer wrapping. Both are made with a polymer based compound. The seats provide the highest value of combustible material because of their size. The seats provided for testing were manufactured by Beurteaux® and are the most common seats used for class 5A spaces, “Ocean Contour 200™.” The foam is made by Dunlop® and the fabric is made by Macquarie®. Both materials meet the fire resistance standards set by UL 1056 which is an approved form of testing for NVIC 9-97 [9]. The seats have a combustible weight of 1.6 kg with a cross sectional area of 0.2 m<sup>2</sup> when projected down to the floor giving a total fire load of the chair at 7.0 kg/m<sup>2</sup>. The seats alone would exceed the limit of 5 kg/m<sup>2</sup> oriented with no space between. But the regulation is for the whole space's fire load over the total area and not specific to each individual item.

The foam used in the seats is not one type. Specific types of foam of varying density and stiffness are used depending on the location to provide extra support or reduce sagging. The specific foam used for majority of the chair is EN 38-200, having a density of 38 kg/m<sup>3</sup> and a tear factor/stiffness of 200 N. Other foams used in seats are EN 50-250 which is used to prevent excessive compression in the seat and EN 36-130 which is used as padding on the back of the seat as seem in Illustration 1. With other foams only accounting for a small amount of the chair, EN 38-200 is used for testing and assumed to be the main contributor of the fire load coming from the foam.



**Figure 1: Ocean Contour 200 seat which specific foam components.**

The upholstery on the seats is available in an assortment of designs and colors. But the type of fabric stays consistent on the seat. The Macquerie® fabric is made up of 60% worsted wool and 40% polyester [9].

The seating material was tested together since this is the way it is constructed on the seats. Initial testing was similar to what was done with the carpet using an outside flame source to see if the material would ignite and sustain a flame. It did not take long for the fabric to ignite and flame. As the fabric released more heat, the foam started to melt and produce volatile vapors. These vapors would then fuel the fire established on the fabric. Eventually there would be enough heat in the sample to where the foam would sustain a flame as a pool fire.

From testing observations, the foam first melts before vaporizing and igniting. The fabric did not melt and quickly ignited and sustained a flame.

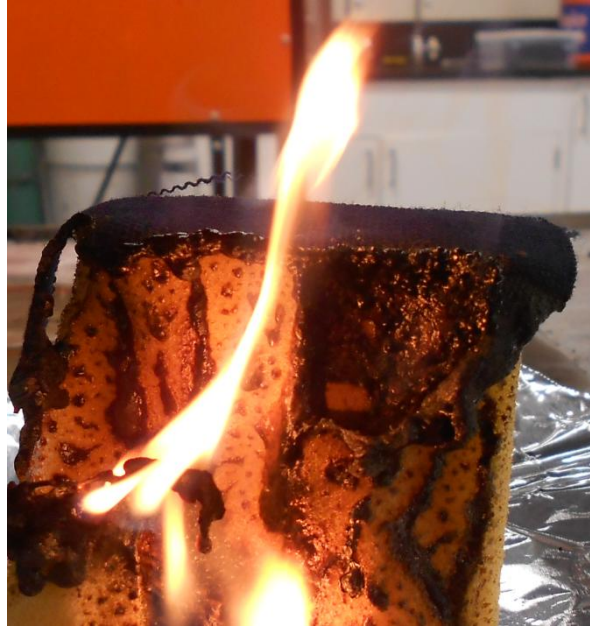


**Figure 2: Foam and fabric sample easily ignited with a light and able to sustain a flame.**

Completing these initial tests show that the seats will be a considerable factor to the fuel load in the space and is likely to initiate the fire. The next step in testing is to determine time to ignition and heat release rate curves which will provide the data needed to create an accurate FDS simulation of the space.

#### Carpet

The carpeting within type 5A spaces must be fire resistant and pass testing according to ASTM E84 which is regulated for ships under 46 CFR 116.423 [10]. The main concern with carpet is its ability to ignite and spread the fire to adjacent combustibles, primarily the seats within the space. Carpet tested was Lees Neofloor™ constructed of nylon fibers and a vinyl backing.

An ignition and flame spread test was conducted on the carpet provided. The initial test conducted was to attempt to create a sustained flame on the material using a simple outside flame source. A hand grill lighter was used on a small strip of carpet.

The carpet took some time to produce a flame and even then it had difficulty sustaining it. Over time the nylon fibers on the top of the material would melt away and cause receded area where the flame of the lighter was. After awhile the under layer vinyl would produce a small amount of vapors and flame.

A flame spread test was then conducted to see if the addition of a flammable liquid would sustain flame. A one by three foot sample was glued down to an aluminum sheet. The initial fuel source came from 25 mL of heptane poured on a three inch by one foot area at one end of the carpet and ignited. The flame quickly extinguished once the heptane was consumed fully. This test was repeated with 50 mL covering a six inch by one foot strip on the other end of the carpet with no sustained flame and no flame spread. The final test used 150 mL of heptane covering the entire carpet sample. This test showed some melting of the nylon fibers but there was no sustained flame or flame spread despite the amount of heat released from the heptane.

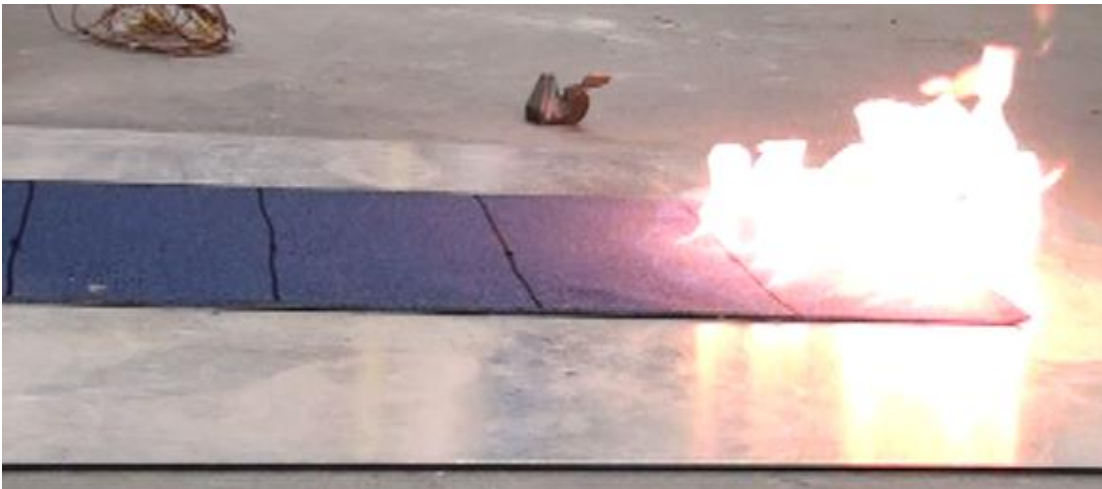


**Figure 3: Flame spread test on carpet using 50 mL of heptane fuel. Only the heptane burned on the surface of the carpet.**

Cone calorimeter tests were conducted after seeing that the carpet can ignite and produce flammable vapors. The initial cone test was at a heat flux of  $15 \text{ kW/m}^2$  with

little effect on the carpet. When heat flux was increased to 20 and 25 kW/m<sup>2</sup>, charring occurred and was more prevalent at the higher heat flux value. No carpet sample ignited in any of these tests despite bringing an open flame to the sample after 5 minutes in the cone.



**Figure 4: Cone samples of the carpet after exposure to 15, 20, and 25 kW/m<sup>2</sup> heat flux in the cone calorimeter. Background carpet was not tested.**

After completing three different tests to determine flammability of the carpet with no success, it is concluded that the carpet will not play any significant role with the fuel load in the space. These tests also support the 46 CFR 116.423 regulation which states carpets must be flame resistant in class 5A spaces.

## Chapter 3: Time to Ignition

### Theory of Ignition

The foam and fabric tested thermally act as a thick solid because of the 5 cm thickness and porous nature. The porous nature makes the foam a heterogeneous mixture incorporating air and its thermal insulating properties. Thermally thick materials have a temperature gradient which can affect the overall time of ignition

depending on thickness. Other way a material can act is thermally thin. Thermally thin materials are considered to not have any type of internal temperature gradient which the physical thickness is less than the thermal penetration depth [11]. A material with a certain thickness will ignite quicker at a thinner dimension than if it was at a thicker size. The samples were tested at a thickness that similar to what is used in the construction of the seats to accurately depict the seat ignition times.

A unique property of the foam and fabric is that it goes through the phase changes from solid to liquid and from a liquid to vapor. The transition through the phases produces a liquid pool fire. Liquid pool fires are unique since the material is amorphous and can spread causing the total surface area of ignitable vapors to increase. The samples were tested in a fixed area tray which prevented the liquid from spreading and allowed it to still be considered solid ignition since the liquid was stagnant.

### Ignition Testing

The cone calorimeter is a powerful tool used for determining specific thermal properties of a material. It uses an array of sensors to determine heat released, mass loss and smoke obscuration to name a few. One of the simplest measurements is ignition time since it only involves a set radiative heat flux in the cone and a timer.

#### Sample

The seat samples were 10.0 cm x 10.0 cm x 5.0 cm in size. Each sample was wrapped with aluminum foil to contain it within the burn dish and prevent leakage out which would lead to inaccuracies. The aluminum protective sleeve was only wrapped to the

height of the burn dish. The reason for this was to account for the foam melting into the dish creating a pool fire and allow maximum exposure. As the foam melted, it would sink down into the dish. By only covering enough of the sample to prevent spillage, the sample is able to be exposed to the cones heat flux without any obstructions.



**Figure 5: Cone calorimeter sample before testing**

#### Cone Calorimetry Testing

Cone testing was completed with an range of heat fluxes to obtain an ignition curve for the seat materials. Fitting a trendline to the data obtain provides a good representation of this ignition curve. 35 tests were completed from 10 to 50 kW/m<sup>2</sup> to provide accuracy of the ignition curve. Most tests were completed at heat fluxes between 10 to 20 kW/m<sup>2</sup> to determine the critical heat flux for the sample. The critical heat flux is the value at which the material will not ignite below. Critical heat flux is important for this experiment because it determines if flame spread occurs across the seats in the space.

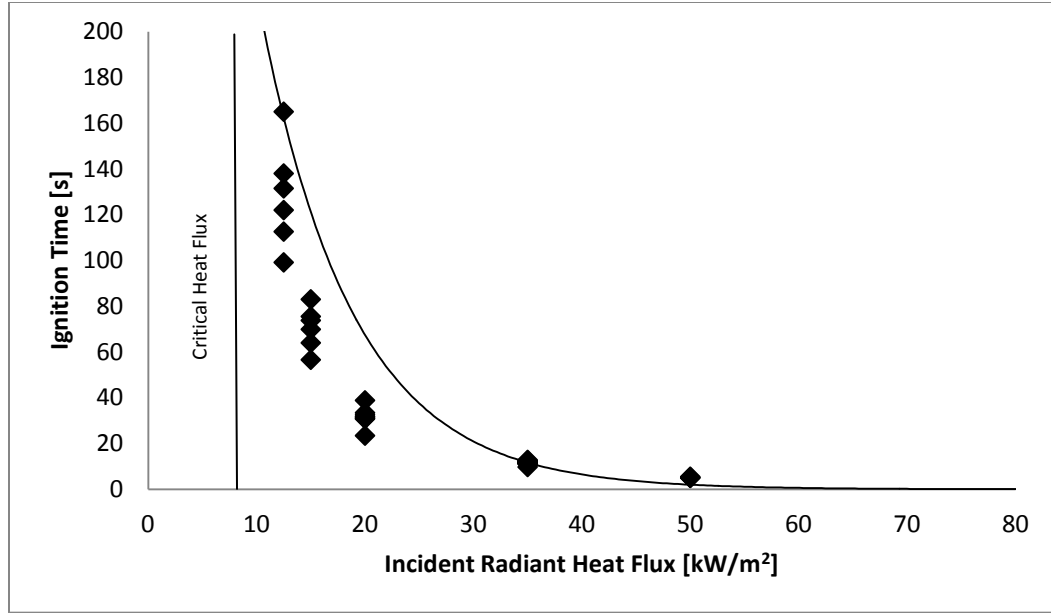


**Figure 6: Time for the sample to ignite to a respective heat flux. Critical heat flux line represents the lowest heat flux value the sample would ignite at.**

The time to ignition exponentially increases to infinity as the radiant heat flux approaches the materials critical heat flux. Figure 6 shows this trend but it is very difficult to determine specific values for certain heat fluxes. The critical heat flux also cannot be accurately depicted from figure 6 or the rough data.

Ignition of thermally thick materials can be accurately determine using [11],

$$t_{ig} \approx \frac{\pi}{4} k \rho c \left( \frac{T_{ig} - T_{\infty}}{\dot{q}''_e} \right)^2 \quad \text{Eqn 1}$$

Equation 1 takes into account the conduction through the materials, temperature at which ignition will occur, and the heat flux the material is exposed to. Time to ignition for thermally thick materials is dependent on the heat flux exposed since the other parameters stay constant for that material. Adjusting the equation to where it only shows a parameter that is a function of ignition that is also directly proportional to heat flux will provide a more accurate predicted ignition times and critical heat flux [11].

$$\frac{1}{\sqrt{t_{ig}}} \sim \dot{q}'' e$$

Eqn 2

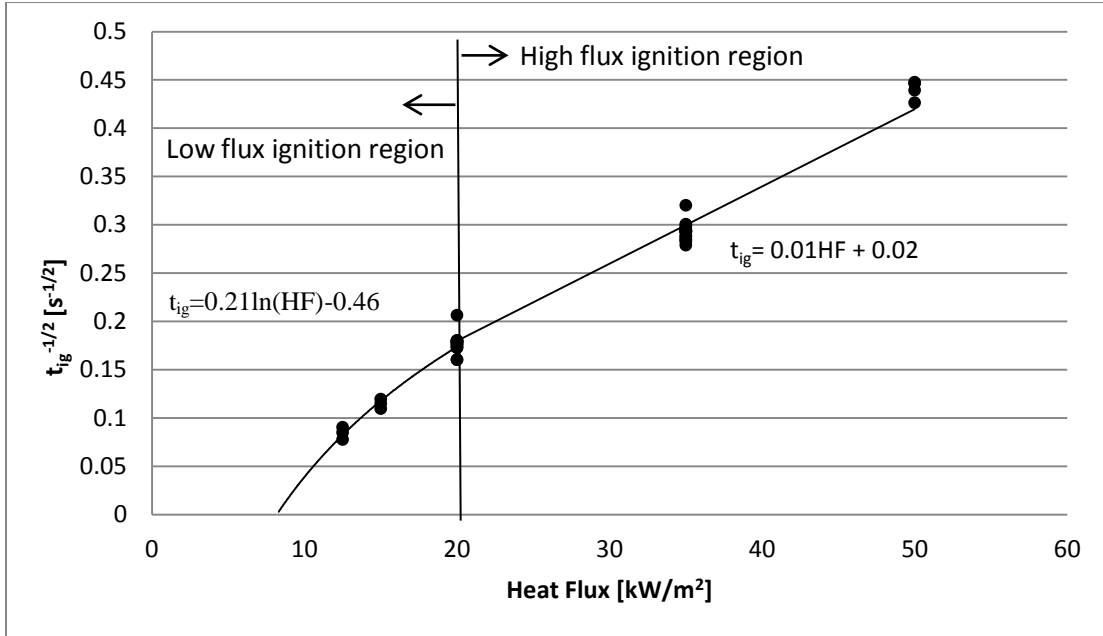


Figure 7:  $1/t_{ig}^{-1/2}$  versus heat flux. Having a more linear representation allows for an increase in accuracy calculating the time to ignition. As heat flux reaches to a critical temperature, this linearity breaks down causing a curve.

Converting the data to this representation increases the accuracy in predicting ignition times for a certain heat flux. Trend lines were used to determine the formulas for the time to ignition seen in figure 7. The trend line is linear for heat fluxes above 20 kW/m<sup>2</sup> having an equation of,

$$t_{ig} = 0.01HF + 0.02 \quad \text{Eqn 3}$$

As the heat flux decreases, the trend line becomes more non-linear until it reaches the x-axis. To extrapolate an accurate trendline, this equation became logarithmic,

$$t_{ig} = 0.21 \ln(HF) - 0.46. \quad \text{Eqn 4}$$

The transition from high to low flux ignition was estimated around 20 kW/m<sup>2</sup>. This value was used since, below this point the samples would not completely burn

shown in figure 8. At  $20 \text{ kW/m}^2$ , the fabric would still ignite and burn. But would produce char that would insulate the foam from the cone's heater and prevent it from continuing to burn.



**Figure 8: Incomplete burn of a sample tested at  $20 \text{ kW/m}^2$  (left) and complete burn at  $50 \text{ kW/m}^2$  (right)**

Around  $10 \text{ kW/m}^2$ , the fabric would sometimes ignite but continue to char over the foam. There was no apparent change in the foam at this heat flux value.

The critical heat flux value is taken at the point the trend line crosses the x-axis. This represents a time of  $\infty$  when converting  $t_{ig}^{-1/2}$  back to seconds. A critical heat flux around  $9 \text{ kW/m}^2$  was calculated using the trend line equation representing the low flux ignition region. A cone test was completed at  $9 \text{ kW/m}^2$  to ensure that the estimated critical heat flux was similar to testing. A couple samples were tested and left in the cone for 30 minutes with no ignition.

## Chapter 4: Heat of Combustion

### Cone Calorimeter $\Delta H_c$ Testing

The heat of combustion of a fuel is the amount of heat released when a unit quantity is oxidized completely to yield stable end products [12]. This value can be measured

in a variety of ways and represent different ways of combustion. Heat of combustion ( $\Delta H_c$ ) was calculated with the use of the cone calorimeter. The cone calorimeter takes the measurements of heat released and divides it by the mass lost to determine  $\Delta H_c$ . The cone calorimeter used for this experiment determines total heat released by measuring the change in oxygen throughout the burning of the sample, known as the oxygen consumption method. This method finds the heat release rate of a sample by measuring the oxygen consumed in a combustion system [5]. Although complex, the practical implementation of the oxygen consumption method is through the following equation for heat release rate:

$$\dot{q} = E(\dot{m}_a Y_{O_2}^a - \dot{m}_e Y_{O_2}^e) \quad \text{Eqn 5}$$

where

$E$  = heat release per mass unit of oxygen consumed (13.1 kJ/g)

$Y_{O_2}^a$  = mass fraction of oxygen in the combustion air (0.232 g/g in dry air)

$Y_{O_2}^e$  = mass fraction of oxygen in combustion products (g/g)

The mass loss rate on the cone is simply measured using a real time scale which measures steps configured by the user.

Taking the heat release rate and dividing by the mass loss rate at that specific time step with the cone will come up with the  $\Delta H_c$  for the sample.

### Sample Heat of Combustion

During every test for time to ignition, each sample was burned till extinguished to determine the  $\Delta H_c$ . 23 of the 35 samples tested provided a  $\Delta H_c$  for the seat sample. The other 12 tests had testing errors related to incomplete combustion or no ignition which caused the values to be scewed beyond practical values for the samples. The  $\Delta H_c$  of the 23 tests are shown below in figure 9.

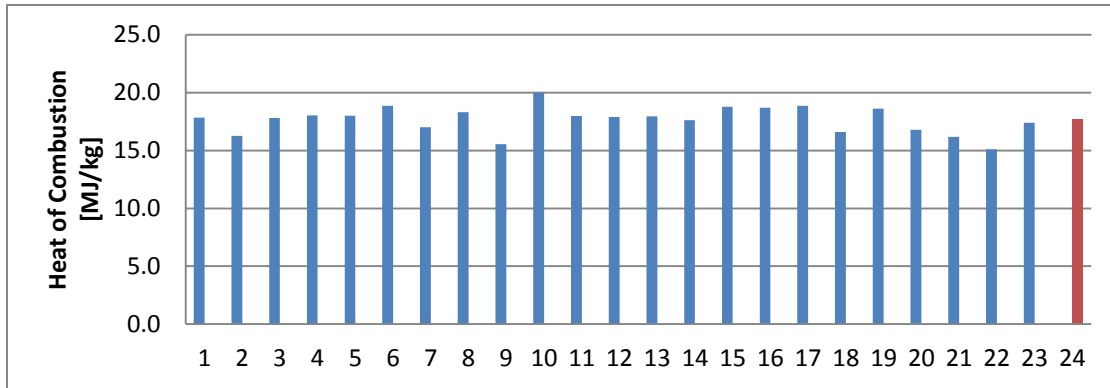


**Figure 9: Graph of heat of combustion for seat samples in cone calorimeter tests. Far right bar represents average of all samples tested.**

Every  $\Delta H_c$  calculated was in the 15 to 20 MJ/kg range with a total average of 17.6 MJ/kg and a standard deviation of 1.17. The cone  $\Delta H_c$  were then verified by completing a theoretical calculation to ensure accuracy. During each cone test, the mass of the sample was measured before and after testing using another scale than the cones. Using these values instead of the cones verify the accuracy. The  $\Delta H_c$  calculated using total mass loss was 17.3 MJ/kg which is close to what was found by the cone.

Determining the  $\Delta H_c$  for the seat sample is important since it is used to calculate the heat release rate of the chairs for the combustion model in FDS. The user is able to set parameters of the combustion model to ensure that the accuracy is in FDS for the specific materials being burned.

## Chapter 5: Heat Release Rate

### Testing Setup

The heat release rate of the chairs will determine if the actual space will reach a critical temperature that would affect the total stay time of passengers on the upper deck. It is important to obtain the most accurate heat release curve as possible in order

prevent any in-congruencies between testing data and what actual occurs. The best way to determine an accurate heat release rate curve for the seats is to complete full scale testing.

Full scale testing was completed by burning a single chair on a scale to determine the mass loss rate. Heat released is proportional to the amount of mass burned and can be calculated using the mass loss rate and heat of combustion. The heat of combustion is assumed to be the same as in the cone calorimeter testing and stay constant through the combustion process.

$$HRR = MRL * \Delta H_c \qquad \text{Eqn 6}$$

#### Setup

The chair was bolted onto a support which was designed to have the chairs height the same as in typical 5A spaces at 0.5 m high. The seat assembly was then placed on top of a burn pan to prevent any material from falling off the scale and causing spikes in the data.



**Figure 10: Seat assembly for full scale testing.**

Heat flux and plume temperature were also measured with mass loss rate to see how these parameters react to the seat burning and to aid in creating an accurate FDS model. Two type K thermocouples were used at heights of 50 and 75 c m above the top of the seat to determine the plume temperature. Three heat flux gauges were used to obtain heat flux readings at a wide variety of distances from the burn seat. These distances represented other seat locations. One heat flux was placed in front facing towards the seats at 45 c m to represent seats in the next row. The other two heat flux gauges were used to represent the seat to the side of the one burning. The orientation and distance to the burning seat depended on the test being conducted. These two gauges represented the seat bottom and seat back and placed at either 7.5 or 22.5 cm away to represent either the seat edge or the center of the next seat. The gauges were oriented at different angles towards the fire to act like the surfaces of the seat.

The seats were ignited using a dish filled with heptane fuel. This ignition source was placed midway to the bottom of the seat from the ground and was supported on its own cradle. This was to prevent the ignition source from being on the scale and causing inaccuracies in the mass loss rate of just the seat. Two ignition points were tested which represent the most likely areas where a fire would occur. The first ignition point tested was in the front of the seat which can be caused from a personal item igniting under the front of the seat. The second ignition point was the side which can either represent a personal item or an adjacent seat on fire. The orientation and distance of the heat flux gauges representing the adjacent seat for each test is shown in table 1.

**Table 1: Adjacent HFG orientation and distance for each test. Asterisk denotes no ignition.**

	Ignition Point	HFG Distance from Burn Seat	HFG Orientation
Test 1*	Middle Front	22.5 cm	Vertical/Horizontal
Test 2	Middle Front	22.5 cm	Vertical/Horizontal
Test 3	Middle Front	22.5 cm	Vertical/Horizontal
Test 4	Middle Front	7.5 cm	Vertical/Horizontal
Test 5*	Side	7.5 cm	45° towards fire
Test 6*	Side	7.5 cm	45° towards fire
Test 7	Side	7.5 cm	45° towards fire
Test 8	Side	7.5 cm	45° towards fire

A total of 8 tests were completed using 5 chairs. Three of the tests resulted in no ignition due to not having enough heptane fuel. These tests were redone with additional heptanes to ensure ignition. In all, 3 seats were completed with a front ignition and 2 seats with side ignition.

## Testing Results

### Mass Loss Rate

The mass loss rate for each seat was recorded using the scale that the seat assembly rested on while testing. The weight obtain represents the whole seat assembly including the pan and legs. These noncombustible materials were not removed since the data is a rate of material burned over time which is only the foam and fabric on the seat. Mass loss rate can be calculated by:

$$MLR = \frac{m_n - m_{n+1}}{t_n} \quad \text{Eqn 7}$$

Equation 5 shows how only the mass burned or lost is accounted for since it takes the difference in masses measured over a certain amount of time. A time step of one second was used in the data logging. The five tests were then plotted to see how the chairs burned.

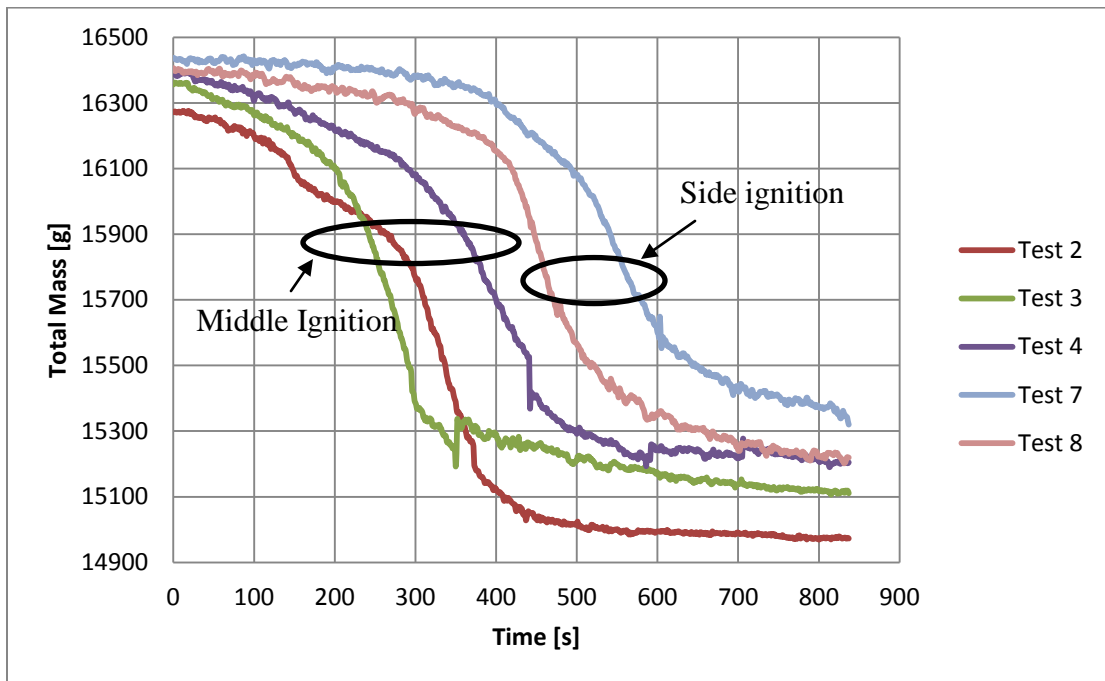


Figure 11: Mass data obtain from the scale. Tests 2-4 represent seats with a middle ignition and tests 7 and 8 a side ignition source.

From figure 11, it is clear to see that the ignition location has an affect the burn rate of the seat. Tests 2-4 were ignited in the middle and 7-8 were on the side. The middle ignition flame spread started in the middle and spread in all directions until the seat was fully burning. Side ignition flame spread only progressed one direction burning from one end to the other of the seat. This process took longer and the reason why the most amount of mass lost in combustion happens later than middle ignition. The spikes and noise in the data came from foam and fabric chunks falling off the seat onto the burn dish and continuing to burn as seen in figure 11.



**Figure 12: Sample chair fully engulfed (left) and a chair after extinguished (right).**

The testing data was averaged to come up with a generic mass loss rate curve for the seat. Each set of data representing a specific ignition source was averaged, due to their burn rate differences. This ensures accuracy of the heat release depending on ignition location.

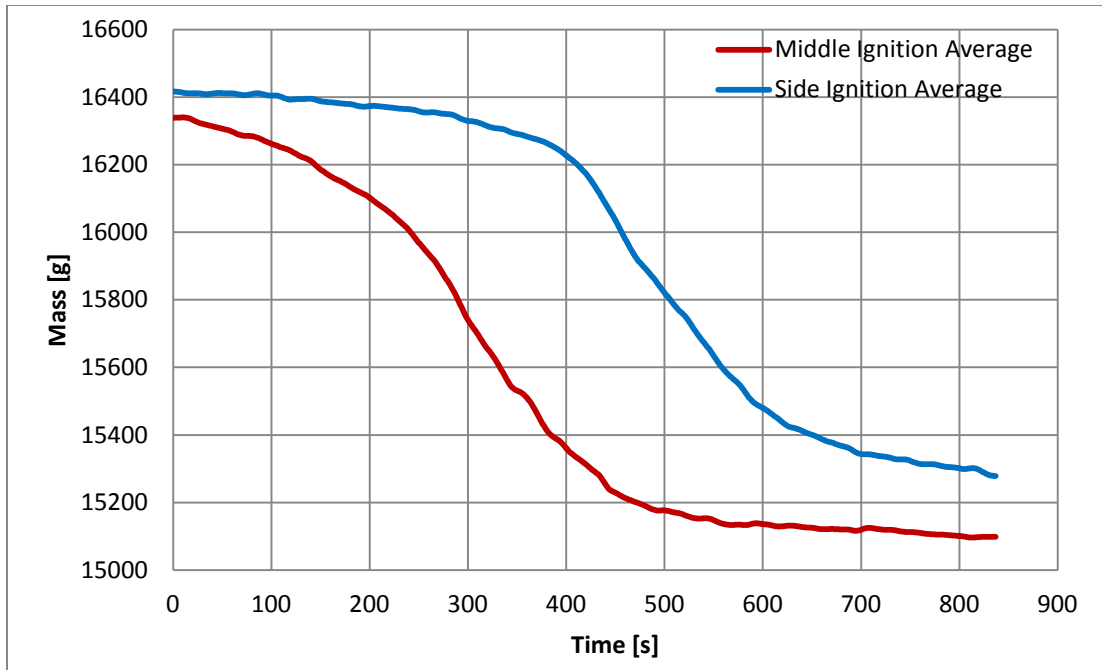


**Figure 13: Average mass loss rate for middle and side ignitions. Middle ignition burned quicker due to faster flame spread across the seat.**

#### Heat Release Rate

The heat release rate for the chairs is the data used in FDS to model a chair burning within the space. Heat released was calculated using equation 6 using the mass loss rate found in the full scale testing and the heat of combustion determined from cone calorimeter testing. Two curves were calculated due to the effect of the point of ignition on how the chair will burn.

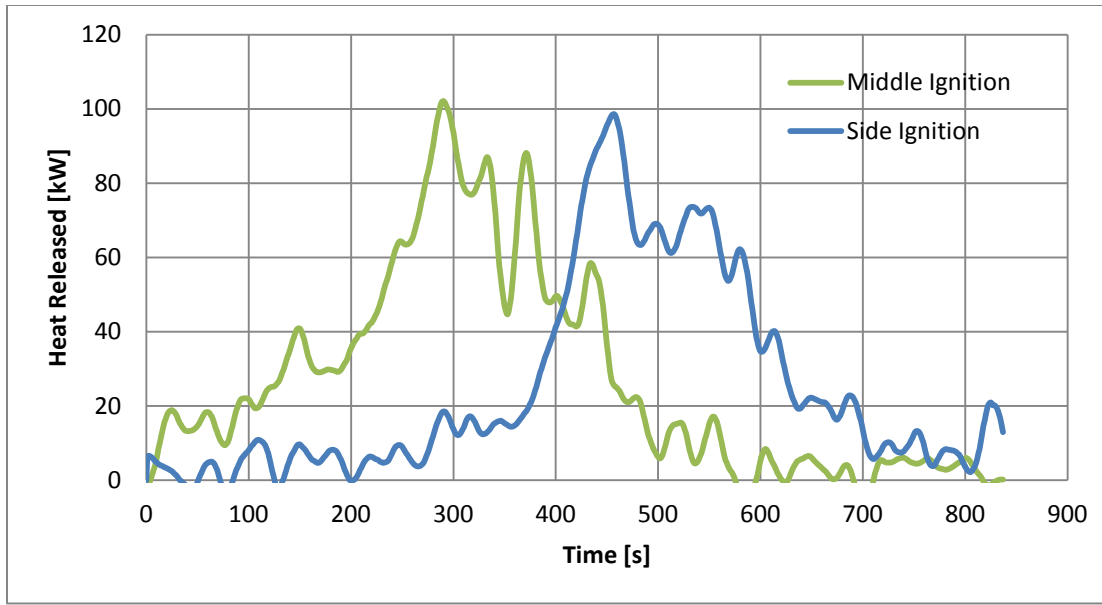


**Figure 14: HRR calculated from MLR and  $\Delta H_c$ . The HRR is proportional to how quickly the flames spread across the chair, making a middle ignition burn quicker but have the same total heat released since all chairs had similar fuel loads.**

The HRR curves show that both chairs have similar curves with the exception of the delay the side ignition has. Each have a growth phase when the flame starts to spread across the seat. The middle ignition spreads quicker since it is spreading from the middle to the edges. The side ignition takes longer since the fire propagates from one side to the other. The peak represents when the back of the chair becomes fully engulfed and heat release rate is 100 kW. The back material only burns for a short time since there isn't much flammable material. This peak heat release rate is verified with video taken of the testing. The seat plateaus after when the bottom cushion continues to burn until no flammable material is left. All seats burned for about 10 minutes but would continue to smolder for some time after.

#### FDS HRR Curves

The heat release rate curves in figure 14 represent the averages of the two ignition source tests completed. These curves still have noise making it nearly impossible to

exactly match in FDS without using thousands of lines to represent every peak and valley. A solution to simplify the curves is to generate a best fit curve of linear segments. Total heat released was used to ensure accuracy of fitted curve by comparing area under each curve. Although the curves may not match exactly, the total heat released from the curve will be retained in the FDS model. Total heat released is calculated by finding the area under the curve.

$$Q_T = \int_{t=0}^{t=b} f(t)dt \quad \text{Eqn 8}$$

f(t)= Heat release rate function

t = time

Since the exact function of the heat release rate is unknown, equation 8 can be converted into a summation of rectangles that fit the unknown curve.

$$Q_T = \sum_{i=0}^{n-1} f(t_i)\Delta t \quad \text{Eqn 9}$$

f(t<sub>i</sub>)= heat released at time step i. (kW)

Δt= time step (s)

The time step is the step at which the scale took readings of the mass which is one second. The total heat released at a specific time step is calculated using equation 9. Summing all these values gets the total heat released for the specific chair.

$$Q_T = \sum_{i=0}^{n-1} HRR_i * t \quad \text{Eqn 10}$$

HRR<sub>i</sub>=heat release rate at time step i. (kW)

t= time (1 second time step)

The average heat released for both ignition points was calculated using Eqn 10 with the heat release rate data obtains from the mass loss rate in testing. Middle ignition had a total heat released of 22.7 MJ and the side ignition had 21.8 MJ. A best fit

curve was then created trying to match each curve as best as possible while attempting to keep the total heat released the same.

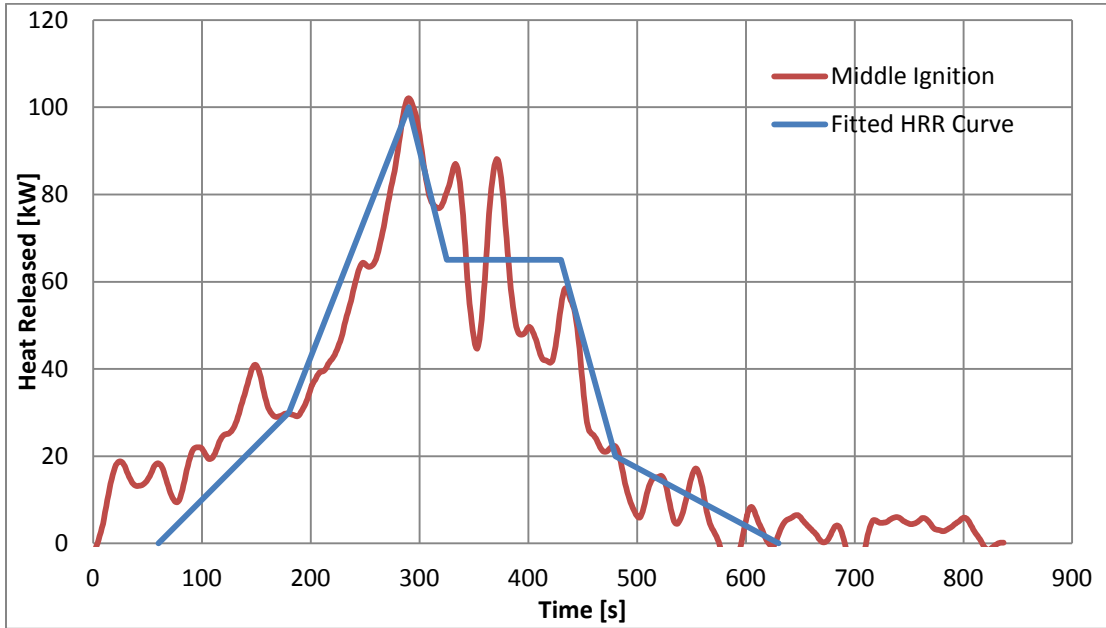


Figure 15: Fitted curve for middle ignition. 1.9% error.

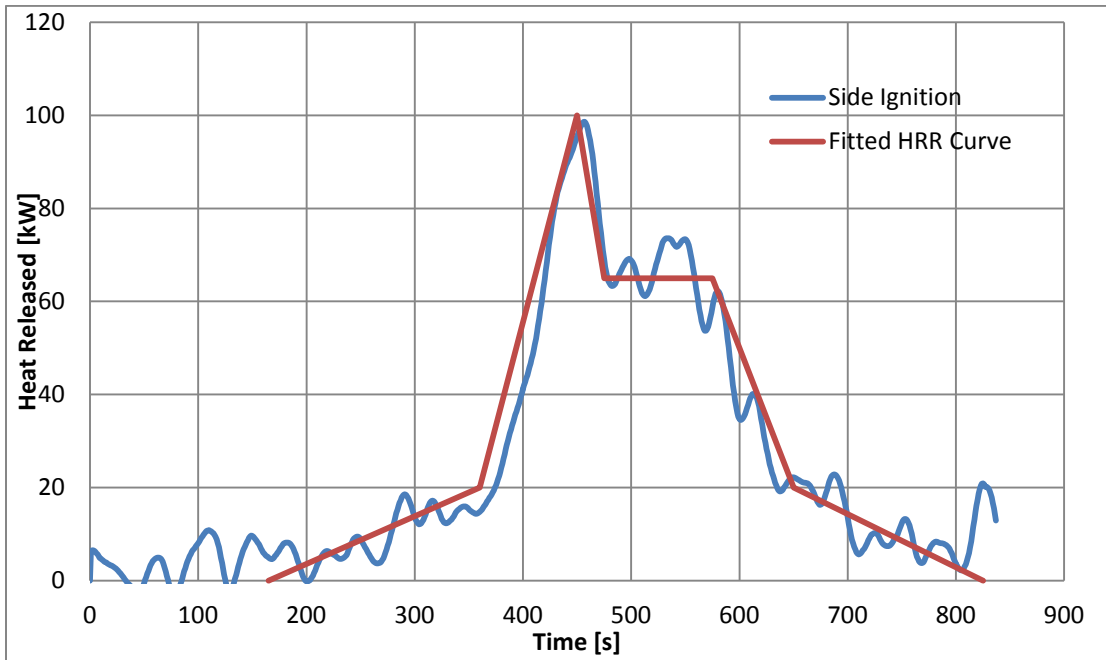


Figure 16: Fitted curve for side ignition. 0.1% error

Figure 14 and 15 show the new fitted HRR curves for both ignition points. Both fit the calculated curve with only being 1.9% and 0.1% off respectively in total heat released from the chairs. The fitted curves will now make it possible to model the seats in FDS with only a few lines of coding. Finding a heat release rate curve for the seat is the final parameter needed for real testing to create a FDS model of the chair.

**Table 2: Fitted curve numerical values set to start burning at time zero that represent a ramp of the HRR of the curves above. The area under the curve was then measured against the total heat released from full scale testing to ensure these values matched.**

Estimated HRR Curve					
Middle Ignition			Side Ignition		
Time	HRR (W)	Q (kJ)	Time	HRR (W)	Q (kJ)
0	0	0	165	0	0
120	30	1800	195	20	1950
230	100	7150	285	100	5400
265	65	2888	310	65	2062.5
370	65	6825	410	65	6500
420	20	2125	485	20	3187.5
570	0	1500	660	0	1750
	Q Total	22287.5		Q Total	20850
	% Error	-1.9		% Error	0.1

Total Q (kJ)	
Tests 2-4	Tests 7-8
22719	20868

## Chapter 6: FDS Radiative Fraction Adjustment

### FDS Model

#### Burn Lab Model

For this experiment, it is crucial that the FDS model matches as close as possible to what can occur in real situations. An exact model of the burn lab was created to adjust

the input parameters describing the fire characteristics. The model's overall dimensions matched the shape and size of the hood with open boundaries to allow smoke and air to exchange freely similar to what occurs in the burn lab. The hood also has a 1 m<sup>2</sup> vent in it which the mass flow rate was determined and placed into the model. Having the vent in the model will allow turbulent airflow to occur which may affect the readings of the thermocouples and heat flux gauges.

Measurement points were placed in the model similar to what was used in full scale testing. Being able to match the readings from the full scale testing will make the FDS model's accuracy more like real situations. Heat flux data points were placed at every location and orientation that was done in full scale testing as well as temperature data points to measure plume temperatures.

The initial ignition source was added since the heat released from this fuel source would affect the readings. The heat release rate for a heptane pool fire was calculated using the mass loss rate and heat of combustion for heptane in a 20 and 30 cm diameter burn dish. The 20 cm diameter burn dish was used for side ignition since it was able to fit under the seat support. The mass loss rate was determined using a scale and the heat of combustion came from literature of 41 kJ/g [11]. Heat released per unit area for the dishes were calculated to be 742 kW/m<sup>2</sup> for 20 cm and 504 kW/m<sup>2</sup> for the 30 cm diameter pan. FDS requires that heat release inputs are per unit of area instead of total value, dividing by the area of the dishes provided the values above [7].

## Chair Model

The model of the chair was simplified down to a simple burner with a specific burn rate. The specific burn rate was determined through the full scale tests for specific ignition points. The HRR curves in figure 14 and 15 were then put into code as burners with fixed heat released at specific times. FDS has the ability to generate a combustion model two ways, either at a specified or not specified rate [7]. Combustion model that burns at a specified rate is the simplest way to generate a fire model for an object since the user determines in FDS how the material burns. The only discrepancy is it removes the unpredictability that fire has with materials. The unpredictability comes as a non-specified burn rate combustion model which requires very specific thermal and physical properties of the material burning. These properties are not known for the compound material of the fabric and foam and would require thermo-gravimetric analysis (TGA) to obtain the data required. The simpler specified burn rate combustion model was used because of full scale testing of the chairs.

The burning of the seat was assumed to mostly occur on the bottom cushion and the burner was therefore only incorporated into this section. The back of the seat was still added since it plays an important part in the fire model since the aluminum can absorb some of the energy and re-radiate it away. The aluminum used to construct the chairs has a specific heat of 0.91 kJ/kg K, density of 2700 kg/m<sup>3</sup>, conductivity of 250 W/m K and a emissivity of 0.75. The emissivity value was set high because of soot accumulation on the chair.

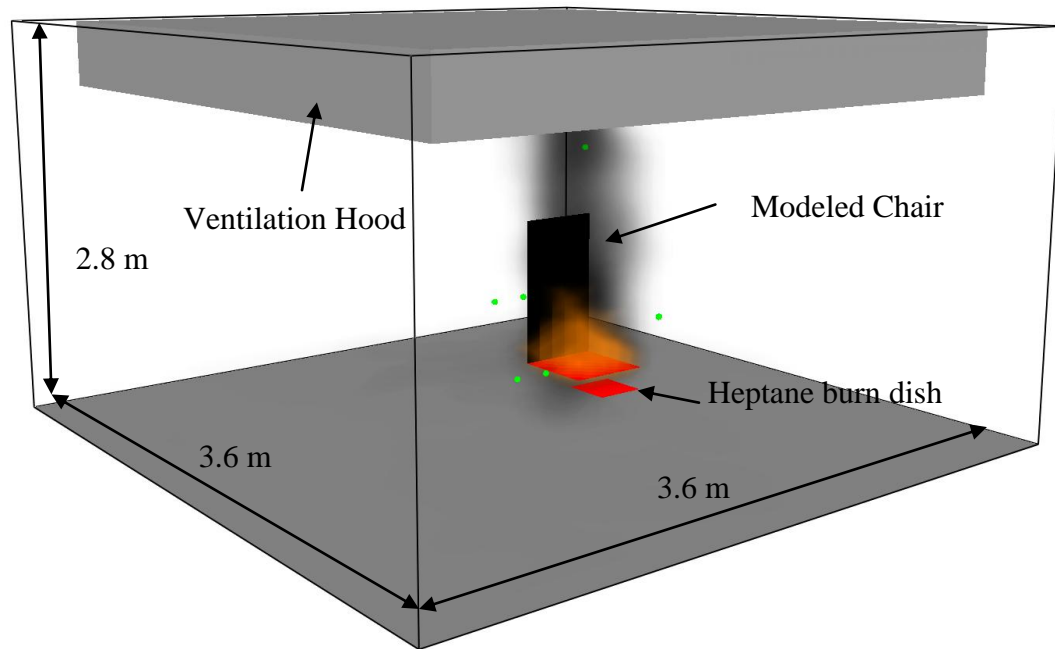


**Figure 17: Small scale FDS model to simulate the burn lab used in full scale testing.**

### Results

The goal for this small scale FDS model was to adjust the model's radiative fraction to match the data from the heat flux data points to the full scale testing. Heat flux gauges determine the amount of radiative heat flux is emitted from a heat source. By default, this value is set to 0.35 meaning that 35% of the heat released from the source is radiation [7]. This default value was determined to be too high and was adjusted until the data matched at 0.25. At a radiative fraction of 0.25, the FDS data was similar in shape and values. Some results are seen in figures 18-20 showing the similarity between the two measurements. Additional graphs can be found in appendix A.

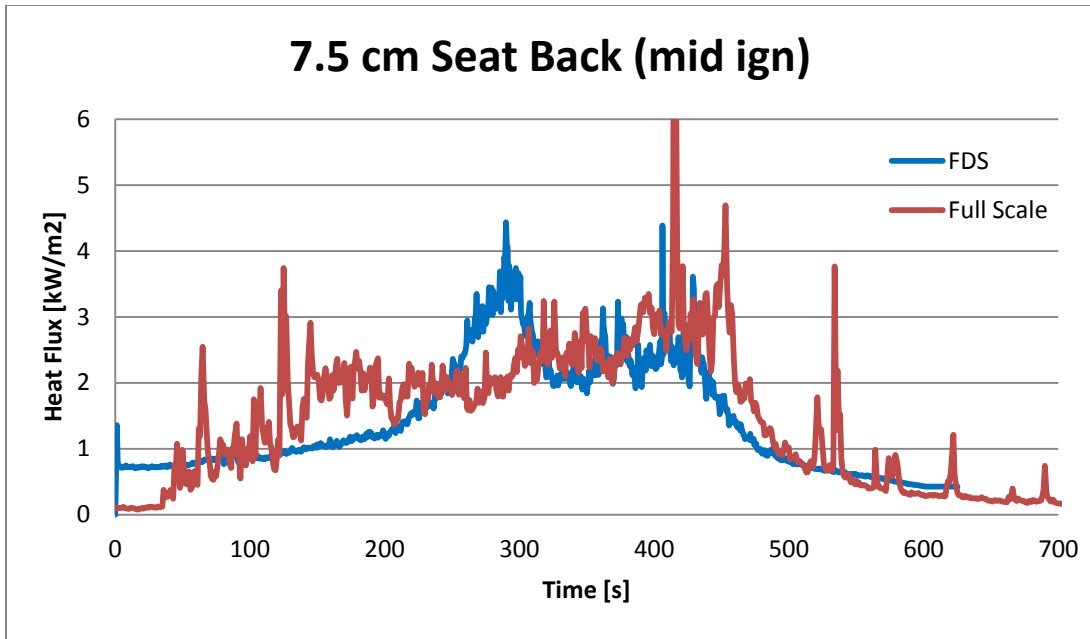


Figure 18: Heat flux data obtains at the back rest of the chair, 7.5 cm away. Ignition source in middle of chair.

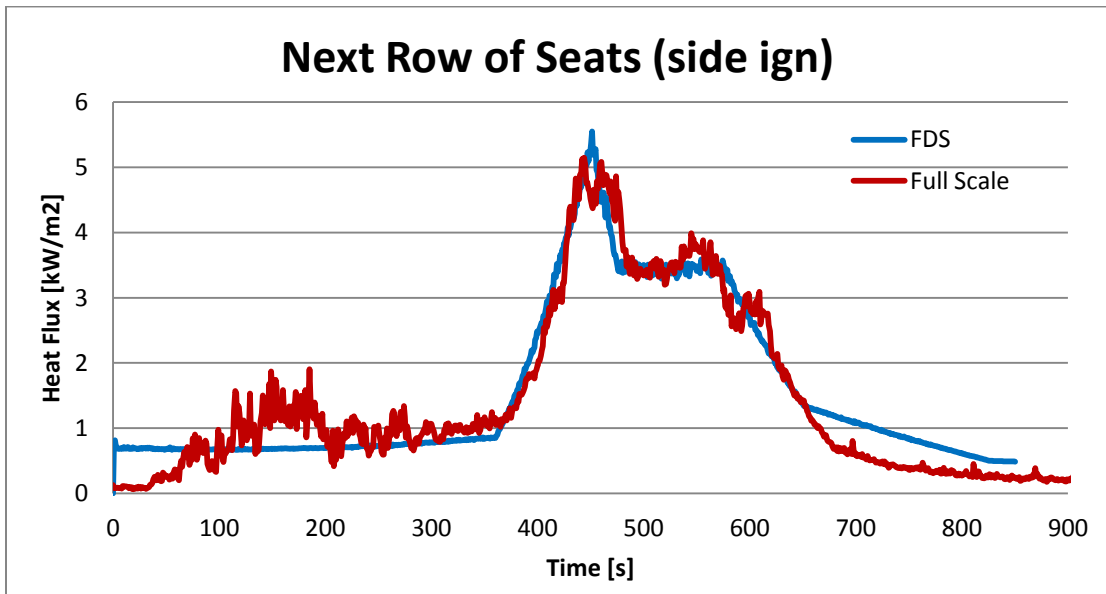
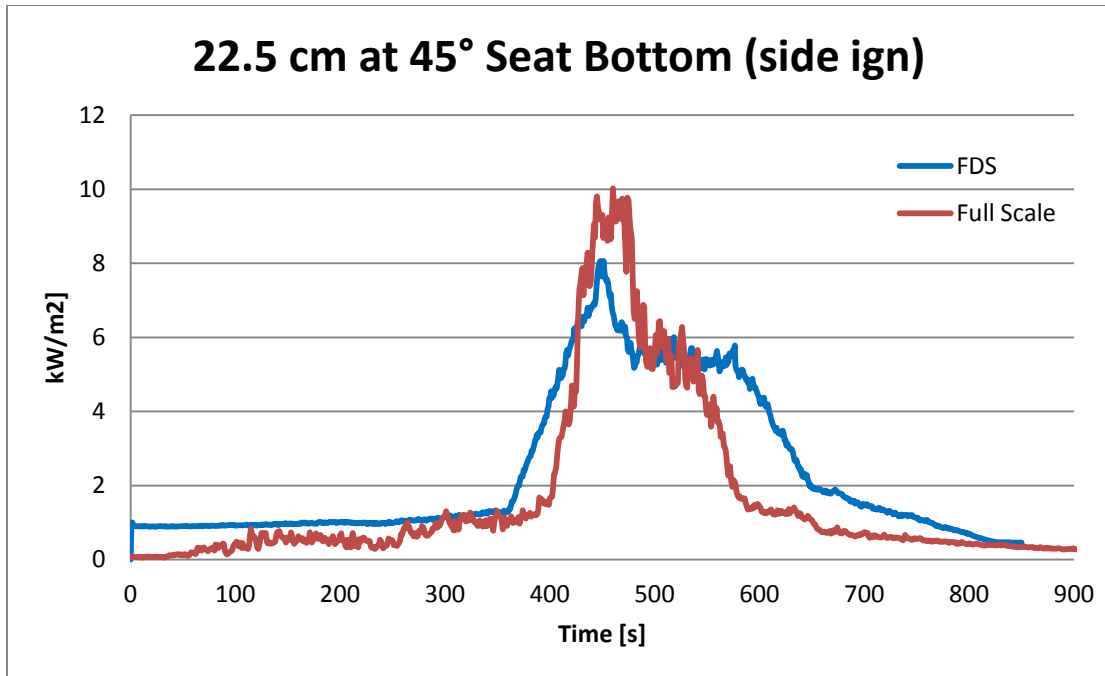


Figure 19: Heat flux data representing the next row of seats fwd of the burning chair. Ignition source on side of chair.



**Figure 20: Heat flux data obtained near the seat bottom cushion 22.5 cm away. Heat flux gauges were tilted 45 degrees towards the burn chair. Ignition was at the side of the chair.**

Some of the data does not exactly match up which can be caused by a number of variables. Some of the results from the side ignition tests show very low values for the FDS model initially. These lower values occur when the heat flux gauge is actually shielded by the seat itself. The cushion heat flux gauges were mounted parallel to represent the adjacent seat surfaces. When the seat burns away, it sinks down to the aluminum support structure. The surrounding foam then blocks the heat flux gauge from obtaining an accurate reading. This was assumed since the other gauges have similar readings to the FDS model like seen above in figure 18. The reason why the FDS model data does not have this is because the thickness of the model is small and does not burn away like in the full scale testing.

## Chapter 7: FDS Full Scale Simulation

### Full Scale FDS model

#### 5A Space

One of the most important parts of this experiment is to create an FDS model accurately portrays a “typical” 5A space. For a space to be considered class 5A, it must meet certain regulations. A vessel which has 5A spaces can only carry 600 or fewer passengers and have no overnight accommodations. 5A space policy is also only suitable for large open public spaces with a uniformly distributed fire load which must be estimated before being classified as 5A [1]. These spaces generally encompass a large portion of the length and entire breadth of the vessel.

The dimensions used in testing were provided by the US Coast Guard Marine Safety Center as part of an ongoing cooperative project between the USCG and the Passenger Vessel Association (PVA).

The space provided had a rough cubic dimension of 26.0 m x 11.5 m x 3.5 m. Some areas were recessed for doorways or for outside walkways. A stairwell is located at the front of the space for access to a 5A space located above. The space above was not modeled for this study since the issue under investigation was only the transfer of heat between the two spaces through the floor with no fire occurring within the upper space. By not modeling the second deck, a reduction of the computational cost of the simulation reduced the amount of time required to run by a factor of hours. A snack bar and head (toilet) space was also added since these things are common for creature comforts. Both of these objects are typically constructed out of aluminum similar to the hull of the ship and were not considered flammable.

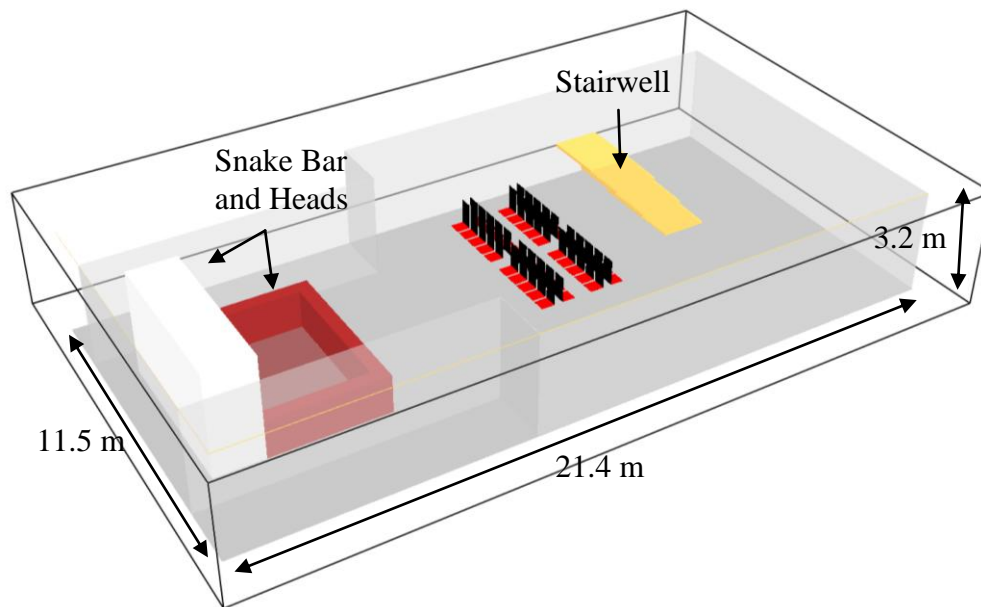


**Figure 21: Model of the 5A space used for testing with labeling and space dimensions. Some rows were taken out to reduce clutter for illustration.**

The bulkheads and decks are constructed with marine grade aluminum having a thickness of 2 cm with thermal properties of 2700 kg/m<sup>3</sup> density, 0.9 kJ/kg K specific heat, and 210 W/m K conductivity. Emissivity was set high at 0.9 due to the soot accumulation from the burning seat. FDS does not typically calculate heat transfer through non-combustible materials and considers these solids to maintain ambient temperature of the sides not exposed to heat [7].

#### Virtual Measurement Points

FDS has the ability to extract specific numerical values in any part of the simulated domain and create a table. FDS uses the Navier Stokes equations at every point in the mesh for calculating the combustion model. To reduce size, these values are not recorded unless desired by the user. The data points added to the model were used to

read temperature and heat flux for the fire spread calculations and boundary temperature.

Heat flux data points were put in locations similar to what was completed in full scale chair testing in order to determine if the adjacent seat is provided with sufficient amount of energy to ignite. Six data points were used in total; two on each side representing the seat cushion and back, one in front and back to represent seats in adjacent rows. These data points representing the seats to each side were placed facing the seat(s) on fire at a distance of 7 cm. The front row point was at 45 cm while the back row was only at 10 cm. The reason for the back heat flux data point being so close is because typically seat rows can be designed to be back to back which concentrates the fuel load and thus can lead to multiple seats ignited at once which is considered a worst-case situation.

Temperature data points were placed on the surface of the ceiling to measure heat transfer through the ceiling to the above refuge space. These points will determine if the upper deck stays within the regulated temperature for stay time that the policy has implemented located at the centerline of the seat fire plume and theoretically measured the highest release of heat in the model.

Other devices used in the model were to assist in creating a visual representation of what was occurring to aid in interpreting the data. These were slice files of temperature gradients which show what the temperature is on a specific plane. It gives a colorful representation of temperature which can be used to determine if additional point temperatures are needed. These slice files only represent the temperature gradient in the air. To visually see the temperature changes in bulkheads

and ceilings, a wall temperature boundary file is used. The wall temperature boundary file shows the temperature on every surface in the model. With the boundaries being exposed, the visual representation of the upper deck temperature is clearly seen.

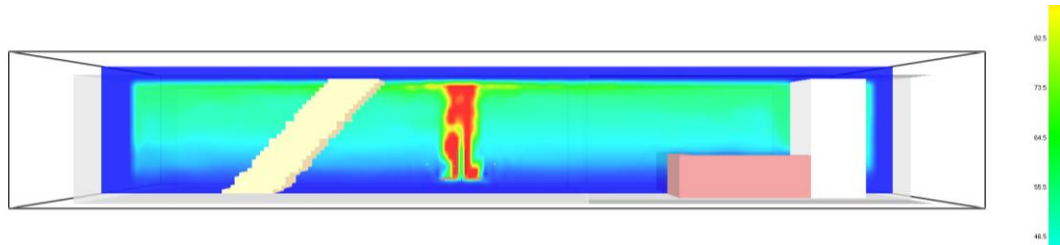


**Figure 22: Profile of the temperature gradient of the air within the space. The fire plume coming from the chairs is distinctly higher than the ambient temperature in the rest of the space.**

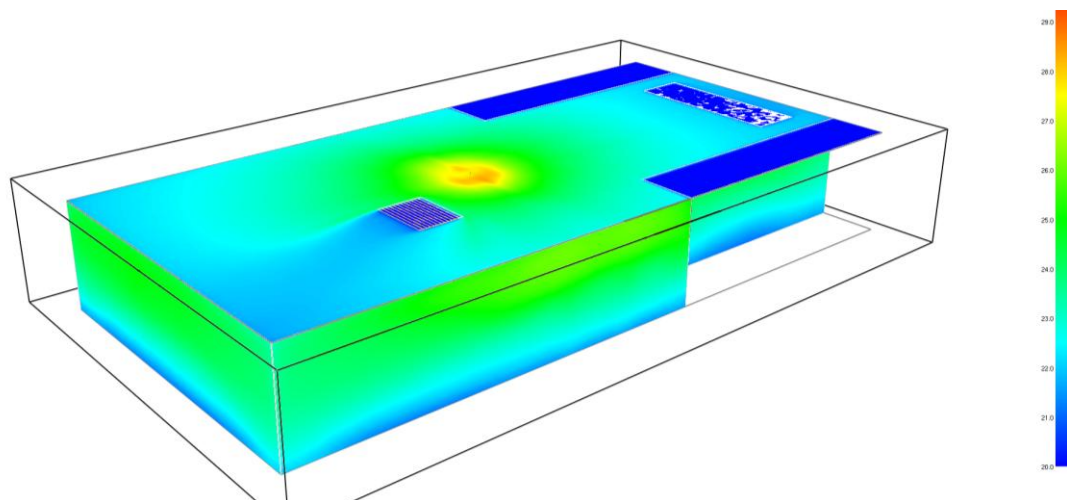


**Figure 23: Temperature gradient of the outer walls of the space. Higher temperatures are centered around where the fire plume's impingement region contacts the wall.**

Other visual representations that Smokeview does by default is soot mass fraction and heat release rate per unit volume. These two visuals represent the flame and smoke generated from the combustion model in FDS.

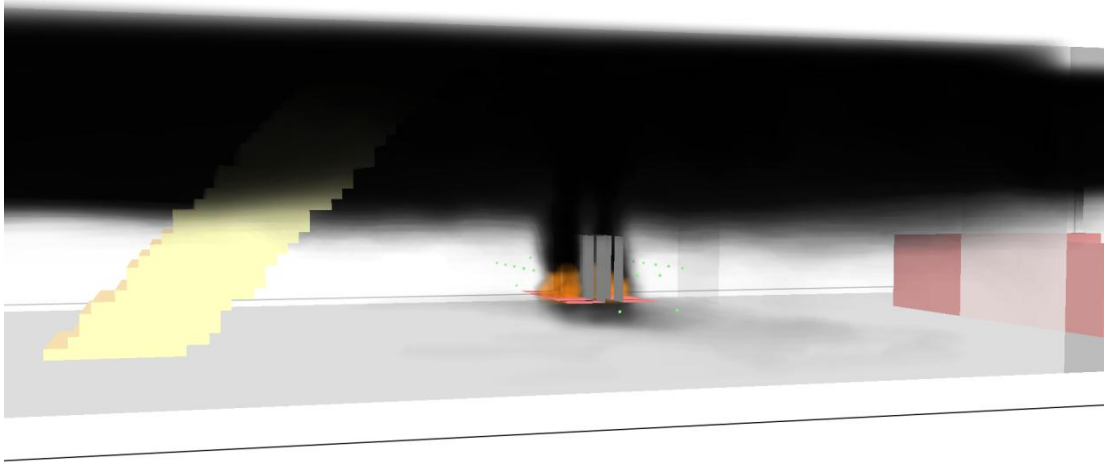


**Figure 24: Smoke layer forming at the upper boundary of the space as the seats burn.**

Full Scale Simulation

Seat Orientations Tested

The seat configuration tested were rows oriented back to back and facing in the same direction. The variety of orientations caused the fire load to change depending on how many chairs were in the simulation. Fire load was calculated for a fixed area depending on row orientation.

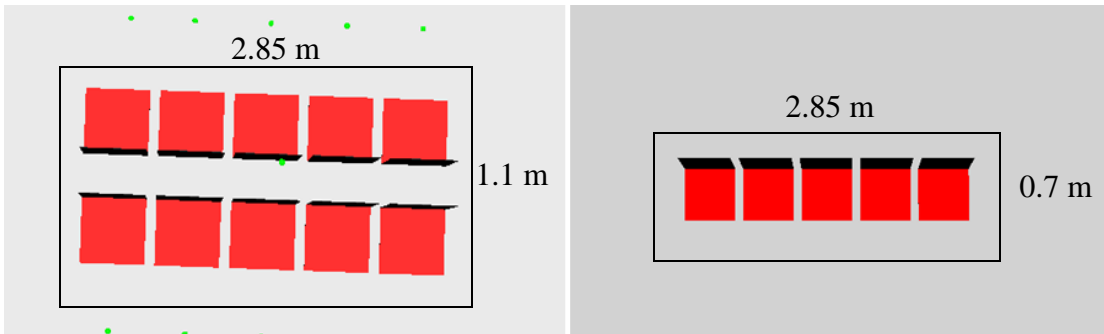


**Figure 25: Fire Load area depending on row orientations. Rows with chairs aligned the same way only require 1 row in area for the module. The box provides area for the seats and aisle room.**

These areas represent the fire load for the whole space since they can be positioned modularly throughout the space. The modules were designed to where only the seats within a single section would burn and have a wide range of fire loads possible in

type 5A spaces. This row configuration is common and represents the highest concentration of fire load due to seats typically found in a type 5A space and would cause the highest anticipated release of energy. Table 3 shows each configuration and the estimated fuel load.

**Table 3: Fire Loads simulated in FDS. Areas vary with how the rows are configured with each other.**

Test Name	Row Orientation	Area (m2)	Fuel Weight	Fire Load (kg/m2)
1 Seat	Same direction	2.1	1.6	0.8
2 Seats	Same direction	2.1	3.2	1.5
3 Seats	Same direction	2.1	4.8	2.3
4 Seats	Same direction	2.1	6.4	3.0
5 Seats	Same direction	2.1	8	3.8
1 by 1	Back to back	3.2	9.6	3
2 by 2	Back to back	3.2	11.2	3.5
3 by 3	Back to back	3.2	12.8	4
4 by 4	Back to back	3.2	14.4	4.5
5 by 5	Back to back	3.2	16	5

The module area is a calculated box that holds rows of 5 seats with space for aisles. Seats oriented the same direction only required 1 row for the module and why the area is lower than the module with 2 rows having the back of the seats together.

The initial ignition point varied depending on the situation that could occur in real life. There are many spaces around the chairs to put bags or other items that could be a possible ignition source. All test ignition points started in the middle of module since this would allow maximum fire to spread. The first ignition point was simple with just having a single chair ignite. The next ignition point was still in the middle of the chair but behind it which would cause both chairs back to back to ignite. Third ignition point tested was between two chairs in the same row. The final ignition point was behind the two rows in the center of four chairs. All the ignition points used the

heat release rate graphs developed during the full scale chair burns. Heat flux was measured around the chairs to determine if any adjacent chairs would ignited.

#### Determining Ignition Times

The alternative to determining whether or not there is sufficient amount of heat to cause ignition of other seat is to calculate it manually and including this information in the FDS input file. This is completed by looking at the heat flux readings obtain from the data acquisition points in the FDS model representing seats around the fire source. Ignition time is calculated by taking the average heat flux over a certain time and comparing these two values to the ignition curve calculated from the cone calorimetry testing. If the exposure time from the FDS model is longer than the time it theoretically ignites on ignition curve for a given heat flux (averaged for the FDS model, but single value for ignition curve), then the seat will ignite. The chair is assumed to ignite at the last time step used for the average. This can be seen visually below from an example in figure 24 and 25.

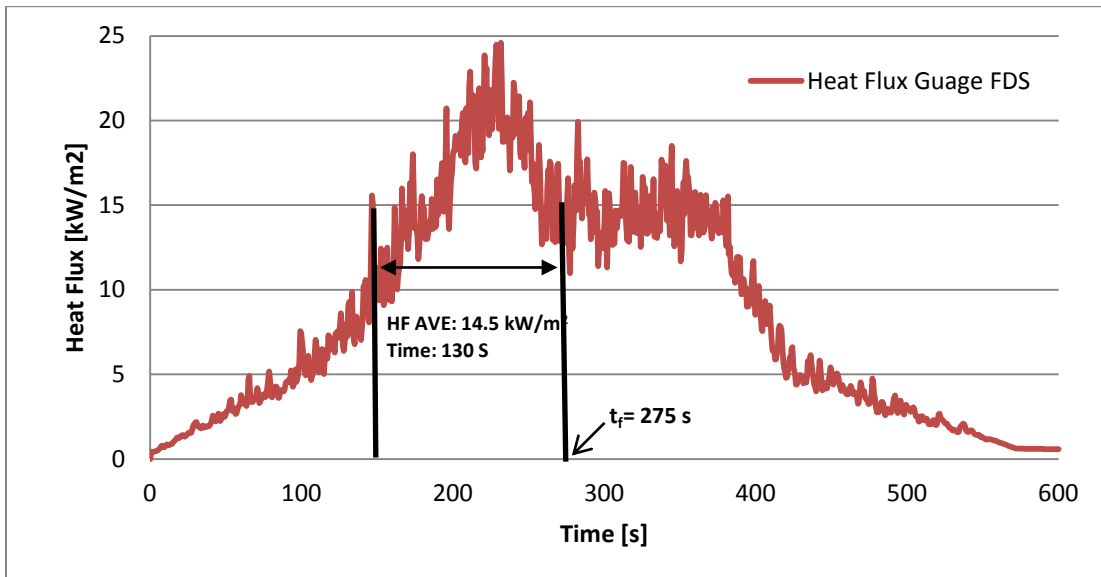


Figure 26: Average heat flux over time. These two values will be compared to what was determine through cone testing. HF Ave 14.5 kW/m<sup>2</sup> over 130 seconds.

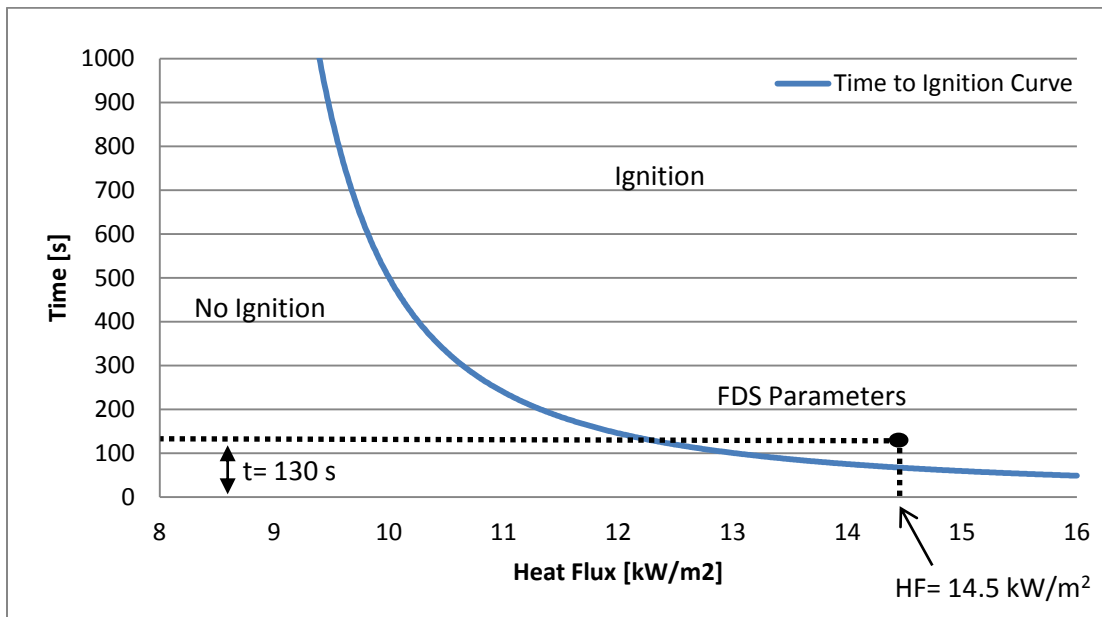


Figure 27: Time to ignition calculation comparing FDS heat flux to the time to ignition curve from cone testing. FDS time is above ignition time for 14.5 kW/m<sup>2</sup>, therefore the seat will ignite at 275 seconds.

These calculations continue until it was determined that there was insufficient heat flux to cause any ignition of additional seats. All the heat flux graphs for each FDS model can be seen in appendix B. Any values lower than 10 kW/m<sup>2</sup> would theoretically take longer than the seats would burn in the model. This helped with determining where the average heat flux should start since it was found that ignition happens around the 14 to 15 kW/m<sup>2</sup> area. Some readings never got above 15 kW/m<sup>2</sup> which means that the average would not come to a value high enough to allow the ignition time to be reasonable. The time it took to obtain an average of 14 to 15 kW/m<sup>2</sup> was close to the ignition time determined in cone testing. Having these two values close together provides a more accurate ignition time for the seat in the FDS model. To complete a full simulation of 10 chairs, a step had to be completed in order to determine when the adjacent seats would ignite. As more and more seats are added

to the simulation, the time of ignition is added to the previous seats ignition time and so forth until no further ignitions occur.

For all the tests, regardless of where the ignition point was, the row with the ignition source did burn completely. For example, the middle ignition single seat simulation was determined to burn all 5 seats in the row. But, it was measured that the heat flux was insufficient to cause the next row to ignite. A reason that this occurred is that the aluminum support back of the seat shielded the next row of seats and prevented sufficient amount of energy needed for ignition. There is foam and fabric on the back of the seat though which could ignited the back of the seat behind. This simulation is accounted for by completing tests with ignition sources between the rows. Seats separated by an aisle as well as rows not back to back did not ignite due to insufficient heat flux. These values never averaged higher than  $5 \text{ kW/m}^2$  which is well below the critical heat flux of  $9 \text{ kW/m}^2$ .

The total heat released into the space progressively increases as more chairs ignite. The maximum amount of chairs that burned was 10 having 5 in 2 rows. Simulating this amount of chairs burning took 3 simulations to obtain. A 10 chair simulation started with 2 chairs in each row igniting simultaneously. This situation could happen if there was a bag between the two rows that would ignite the chairs. Both chairs in FDS are simulated as having a middle igniting and the total heat released into the space is the sum of these fixed heat release ramps.

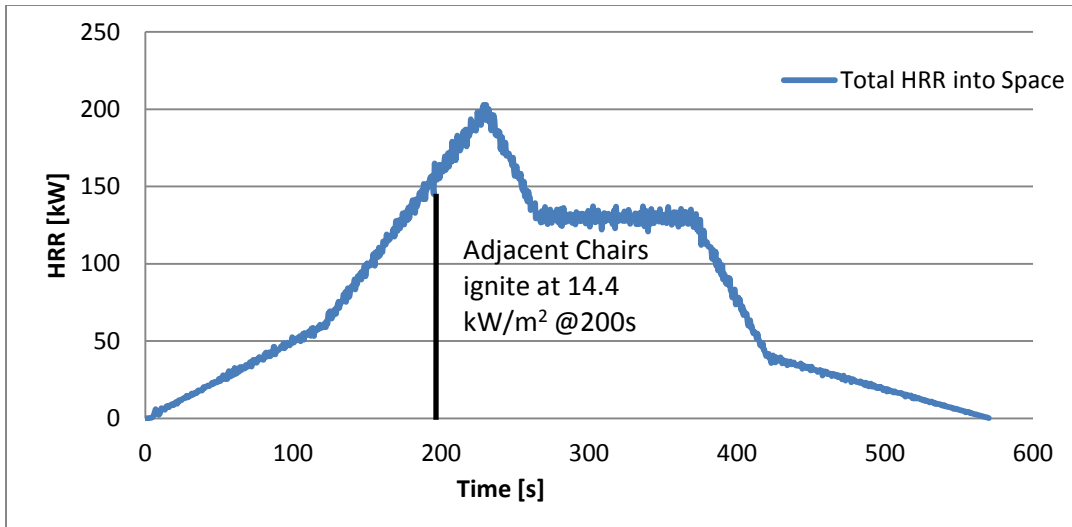


**Figure 28:** Total heat released by two chairs burning at the same rate. This rate simulates a chair with an ignition source at the middle of the seat. As more heat is released the adjacent chairs ignite.

As the two chairs fire growth increases, the total heat released progressively ramps up. This heat eventually ignites the adjacent chairs at 200 seconds after the initial ignition. Since the ignition occurs at the chairs in the middle of the row, chairs on either side ignite bringing the amount of chairs burning to six.

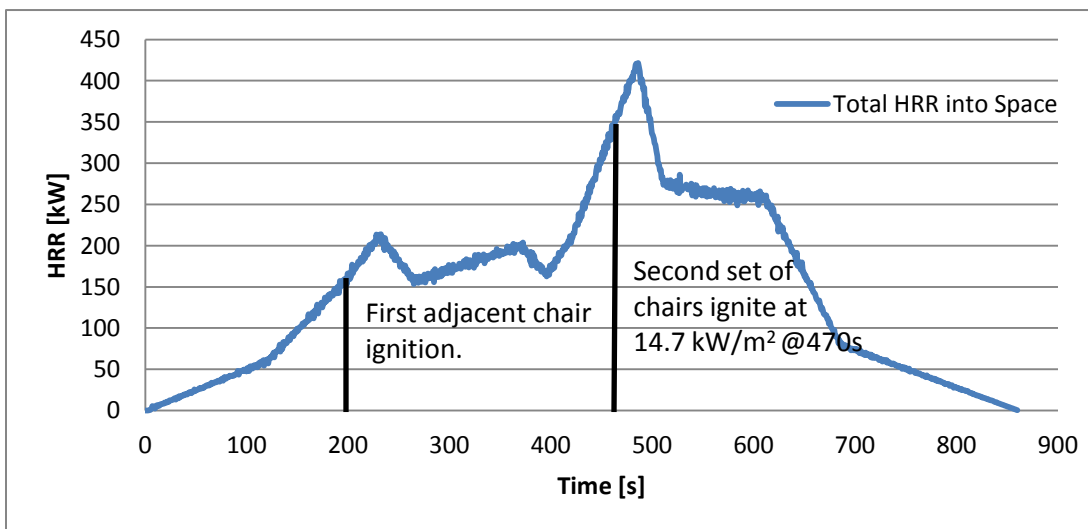


**Figure 29:** Total heat released by six chairs burning. The adjacent chairs ignited have the side ignition HRR curve since ignited by adjacent seats.

The chairs ignited used a side ignition heat release rate profile and brings the total to six burning chairs. Eventually the last two pairs of chairs ignite at 470 seconds giving

a total of 10 and the whole section of chairs on fire. The final breakdown of total heat released by the amount of chairs burning can be seen in figure 30. The ignition steps on when the seats ignited is visualized in figure 31.

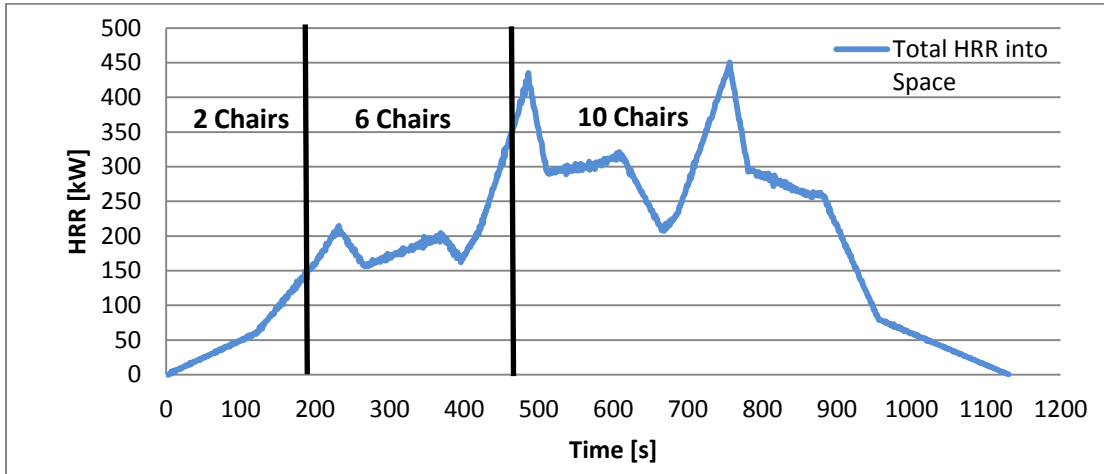


**Figure 30: Total HRR with chair ignition points (black lines) and amount of chairs burning.**

The 10 chair model was used to simulate a conservative fire spread in a section of seats by allowing multiple ignitions to occur simultaneously over the maximum amount of chairs possible. No other chairs outside this section ignited since the heat flux across aisles and rows (with the exception of chairs being back to back) was not high enough for ignition.

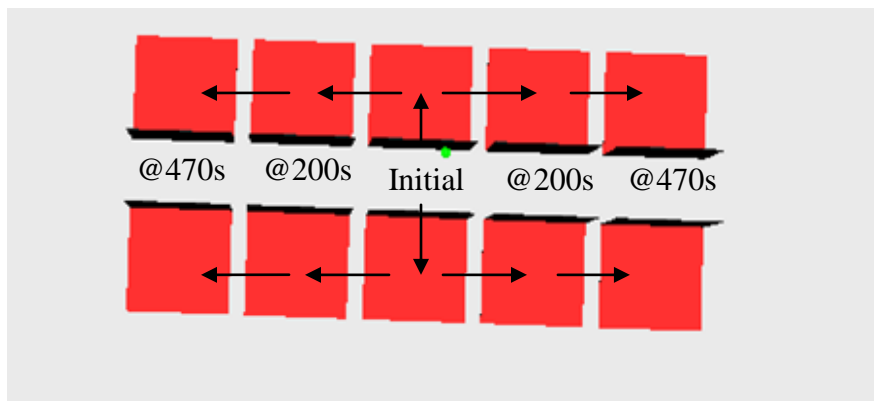


**Figure 31: Visual of fire spread across the 10 chairs. No other seats in other aisles or rows ignited since heat flux was below the critical value.**

Since all the chairs do not ignite simultaneously, the total heat released into the room does not reach a theoretical max value of 1 MW (10 chairs with max HRR of 100 kW each). Instead it only reaches 450 kW. This total heat released into the room has a direct correlation with how quickly the upper aluminum ceiling temperature rises.

### Deck Temperature

Each test had the temperature measured at the center of the fire plume. The temperature devices took readings of the upper and lower side of the deck. The 10 chair orientations were tested and deck temperatures were measured for each. The times of each test varied with how long it took to burn off the chairs in the test. Each test represents fire spread to adjacent seats until all seats were consumed.

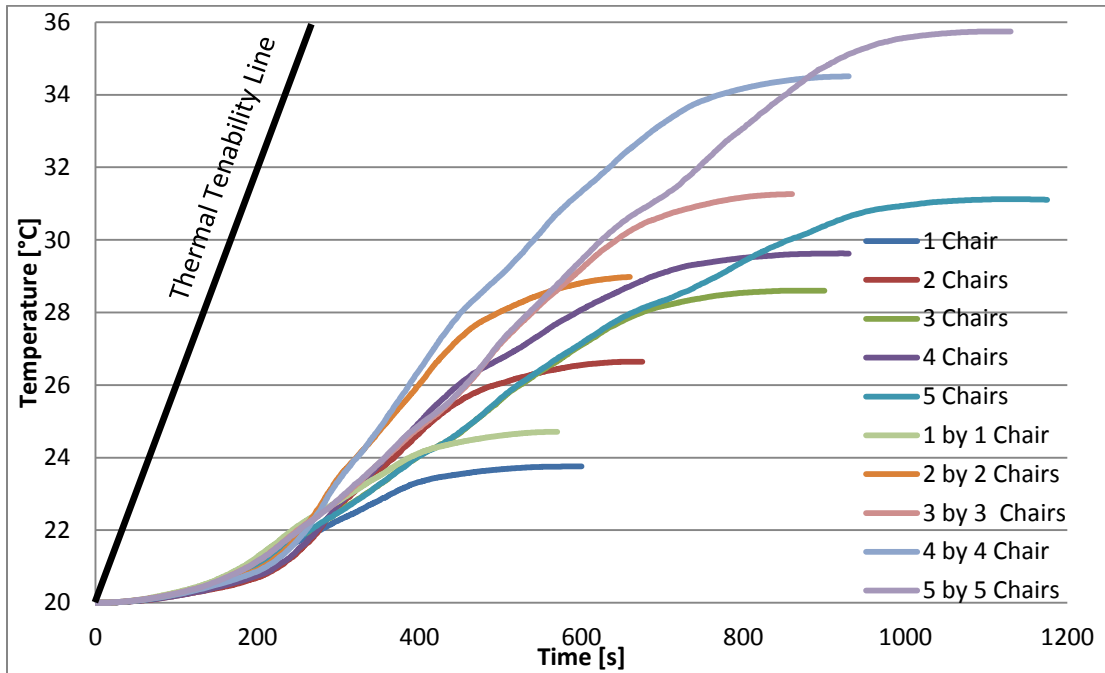


Figure 32: Upper deck temperatures from FDS testing.

Figure 32 shows the 10 tests completed in FDS. The graphs labeled X by X mean the number of chairs of each row burned in the test. It is clear to see that the test that burned all 10 chairs had the highest temperature increase. One promising observation

from this data is that the highest temperature found on the upper deck was only about 36° C. This is well below the critical value of 232° C when aluminum's structural integrity is affected. The linear line shown on the graph is the theoretical thermal tenability line. This line represents a first order equation that represents the ramp from 20° C (@ t=0 s) to 232° C (@ t=3600 s). As long as the upper deck temperature remains below this value, passengers standing on the deck above can remain for the entire one hour [1]. If the temperature ramp is higher, there is a possibility the aluminum will reach a critical temperature and structural integrity will start to become a factor before the 1 hour stay time has elapsed. It is clearly evident that the deck temperature stays well below this line and does not exceed a value above 36° C.

## Chapter 8: FDS Model Adjustments and Corrections

### Mesh Size Adjustments

Mesh size of the boundary can cause the biggest change to accuracy to the output parameters. The mesh size can affect how the calculations occur within the model. The finer the model mesh is, the more calculations per time step occur and theoretically the accuracy of the model increases. Unfortunately the most significant limitation to the model's mesh size is the computer used to process it. The perfect model would be able to have infinitely fine mesh size allowing calculations to occur at the atomic level. But to this day, computer power has yet to reach this accuracy. Standard desktops were used in this study since access to super computers was limited.

The best way to determine a good mesh size for FDS calculations without causing high amount of computation cost is by relating the mesh size to the characteristic fire diameter [7]:

$$D^* = \left( \frac{\dot{Q}}{\rho_{\infty} c_p T_{\infty} \sqrt{g}} \right)^{\frac{2}{5}} \quad \text{Eqn 11}$$

$$\frac{D^*}{\delta x} \quad \text{Eqn 12}$$

Where:

- D\* = characteristic fire diameter
- Q = heat release rate (kW)
- $\rho_{\infty}$  = density of air (kg/m<sup>3</sup>)
- $c_p$  = specific heat capacity of air (J/kgK)
- $T_{\infty}$  = ambient temperature (K)
- G = gravity (9.81 m/s<sup>2</sup>)

Setting equation 12 to a specific value determines how refined the mesh size is. The higher the value, the finer the mesh will become. This value is completely determined by the user but testing by the US Nuclear Regulatory Commission for validation purposes has determine that fire plumes can be adequately resolved if the ratio is between 4 and 16 [13].

Initial model simulations were estimated at a max heat release rate of 400 kW. This value was used instead of the theoretical max release rate of 1 MW because the chairs do not burn all at the same time. Max heat release rate of 400 kW gives a characteristic fire diameter of 0.665 which can then be used to determine a mesh size suitable for simulation. The max heat release rate was confirmed by running a model with 10 chairs in which the max heat release rate was at 450 kW.

For previous simulations, a  $D^*/dx$  value of 4 was used giving a mesh size of 6.6 cm with 291,600 cells. Although this may be considered adequate [13], increasing this value will further increase the accuracy of the model. This ratio was increased to 10 for a simulation to see how temperature, radiative, and convective forces at the center of the plume on the lower surface of the upper deck changed with a finer mesh. The mesh size at this ratio has a cell size of 4.15 cm with 4.6 million cells. This is an increase of 16 times over the coarse mesh.

The model used previously for full scale testing was altered to determine more specific parameters dealing with convection and radiation from the fire plume and the upper deck. The 2 by 2 chair configuration was used instead of the 5 by 5 to reduce computational cost and overall computing time of the model. Saving 100 seconds in the model can correlate to a couple hours saved in compute time. This model's fire plume is also the most symmetric since all chairs are burning at once equal distances apart.

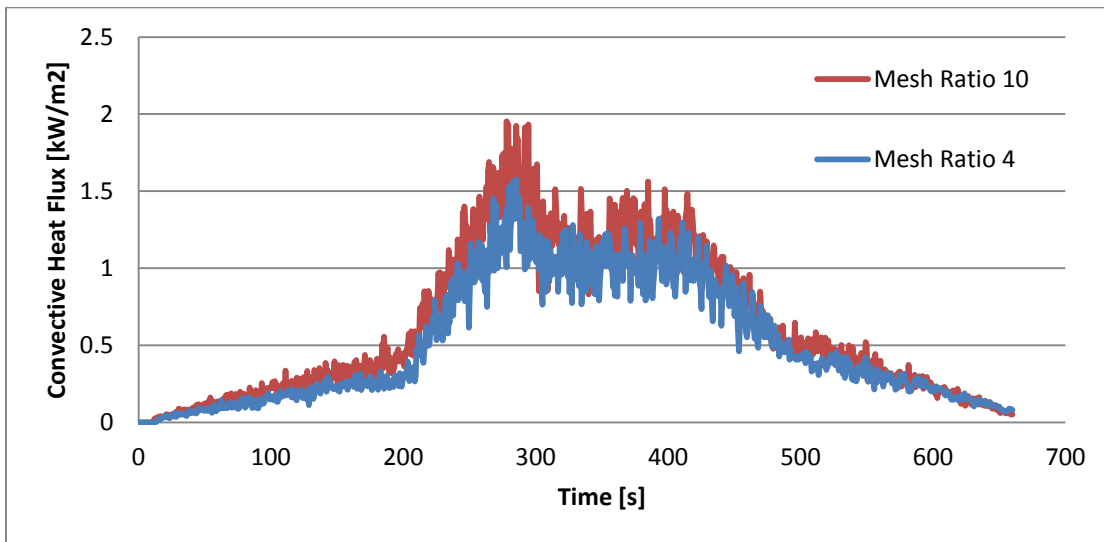
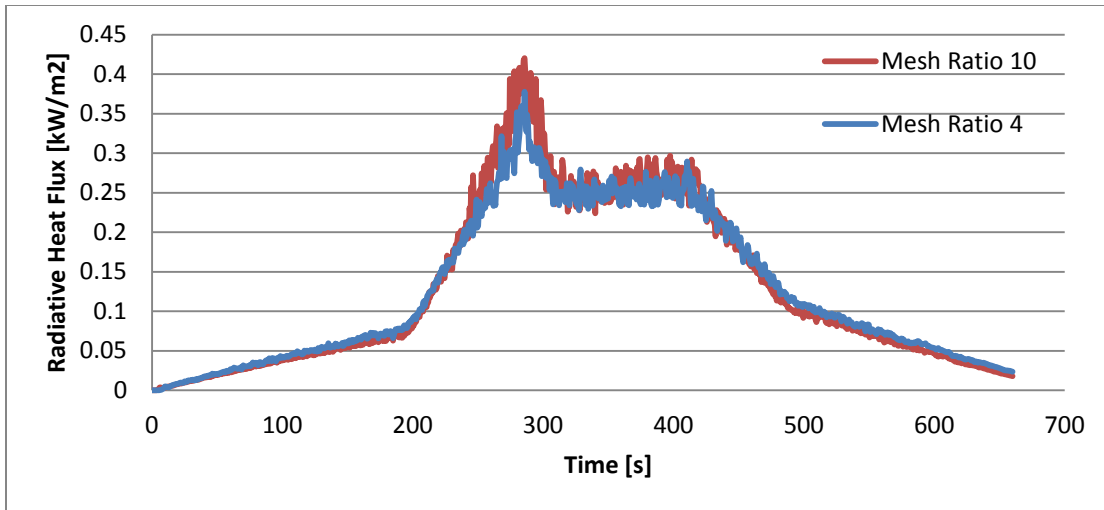
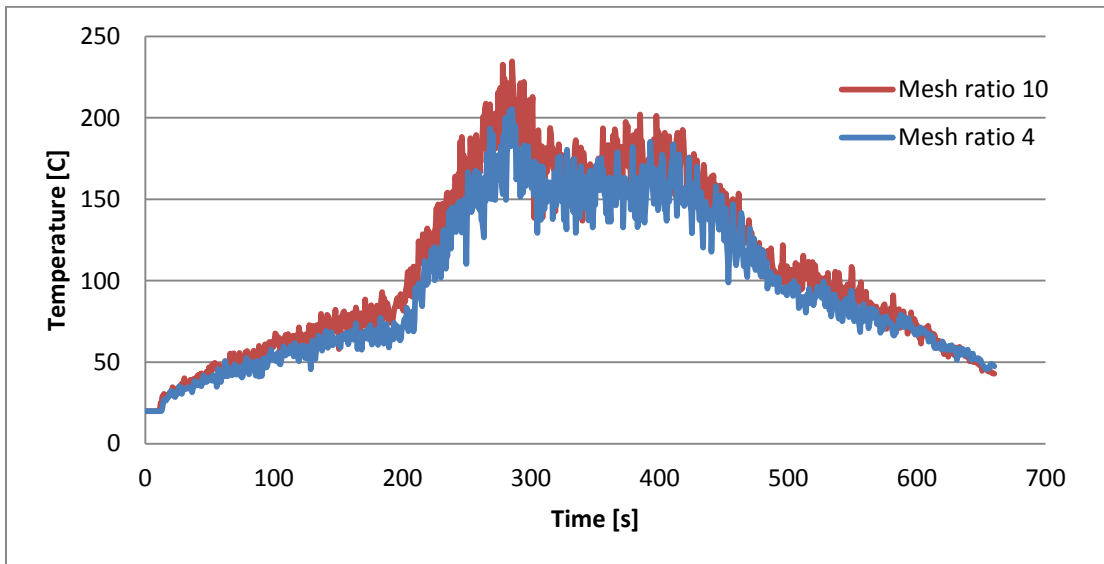


Figure 33: Convective heat flux comparison of mesh sizes.



**Figure 34: Radiative heat flux comparison of mesh sizes.**



**Figure 35: Temperature difference between mesh resolutions**

The values from the two mesh sizes are very similar with only being a few percent off. The amount of time to calculate each was 2 hour for the  $D^*/dx=4$  and 40 hours for  $D^*/dx=10$ . Using the finer mesh with 16 times more data points did not increase accuracy enough to justify the 20 fold increase in computation time.

### Conduction

At this point the addition of a insulator to the upper deck was added to simulate the carpet typically installed on the decks surfaces. The thermal properties of the carpet were conservative with typical insulations with specific heat 1.5 kJ/kg K, conductivity of 0.05 W/m K, and density of 1000 kg/m<sup>3</sup> [22]. The carpet's thermal properties cause the upper deck to retain most of the energy from the fire instead of losing it to the surrounding air. The carpet was not added to previous tests since it was desired to see if bare aluminum deck would reach critical temperatures. Since it did not, breaking down the model into specific thermal parameters help validate the testing.

### Convection

An important aspect of this testing is to ensure that proper heat transfer is occurring from the air to the surface of the upper aluminum deck. This is also the most difficult for FDS to calculate thermal boundary conditions due to the limitations in the model algorithms or resolution of the numerical mesh [7]. FDS uses Large Eddie Simulation (LES) calculations for modeling heat transportation. It accounts for both natural and forced convective heat fluxes onto a surface with the correlations [7]:

$$\dot{q}_c'' = h\Delta T \frac{W}{m^2} ; h = \max \left[ C_1 |\Delta T|^{\frac{1}{3}}, \frac{k}{L} C_2 Re^{\frac{4}{3}} Pr^{\frac{1}{3}} \right] \frac{W}{m^2 K} \quad \text{Eqn 13}$$

where:

$\Delta T = T_{\infty} - T_w$

$C_1$  = natural convection coefficient (1.52 for horizontal and 1.31 for vertical, by default)

$C_2$  = forced convection coefficient (0.037 by default)

$L$  = characteristic length of the plume to the size of ceiling

$k$  = thermal conductivity of air

$Re$  = Reynolds number

Pr = Prandtl number

FDS calculates most of the values that relate to dimensions and forces within the model by default. But the empirical coefficients can be changed to alter the value of convective heat flux of the model. This is important since the majority of the heat flux transferred into the upper deck comes from convection.

A convective heat flux data point was added to the wall in the centerline of the fire plume to verify that FDS has the proper convective coefficient values. The plume in these tests is considered weak since the flame height is much less than the height of the ceiling above the burning fuel [14]. Flame height can be calculated using Heskestad's equation for characteristic flame height [15]:

$$L = -1.02D + 0.235\dot{Q}^{2/5} \quad \text{Eqn 14}$$

where:

L = flame height, m

D = diameter of fire source, m

Q = total heat release rate, kW

Using equation 14, the flame height of the chairs is 1.47 m. A diameter of 1.085 m was used by converting the area of the square chair area to circle to determine diameter. Total heat release rate was the sum of the max heat release rate of the four chairs which comes out to 400 kW. The flame height originates at the bottom of the seat which is 0.5 m above the bottom surface of the model. Correcting the flame height to originate at the bottom of the model gives a flame height of 1.97 m. Comparing this to the overall height of the space at 3.5 m shows that the flame does not reach the upper surface and is thus a weak fire plume.

The correlation to ceiling jets and heat flux to a surface for weak plume-driven flow field was determined by Ronald L. Alpert [16] and experiments of Yu and Faeth [17].

They came up with correlations which determine the convective heat fluxes within the impingement (turning) region and ceiling jet region. The impingement region is the region where the fire plume alters its direction from vertical flow to horizontal across the surface [14]. Since the device used in the FDS model was located at the center of the fire plume, it resides in the impingement region and not the ceiling jet region (r=0).

Yu and Faeth conducted experiments with small pool fires to determine a correlation for convective heat flux to the ceiling in the impingement region [17]:

$$\frac{\dot{q}'' H^2}{\dot{Q}_c} = \frac{31.2}{Pr^{3/5} Ra^{1/6}} = \frac{38.6}{Ra^{1/6}} \quad \text{Eqn 15}$$

$$Ra = \frac{g \dot{Q}_c H^2}{3.5 \nu^3} = \frac{0.027 \dot{Q}_c H^2}{\nu^3} \quad \text{Eqn 16}$$

where:

- $q''$  = convective heat flux, kW/m<sup>2</sup>
- $\nu$  = kinematic viscosity of air, m<sup>2</sup>/s
- H = height of ceiling, m
- $Q_c$  = Convective heat release, kW

Equation 15 has been established for plumes with Rayleigh numbers from 10<sup>9</sup> to 10<sup>14</sup> [14].

Alpert also conducted experiments at higher air pressures to allow the Rayleigh number to exceed 2 x 10<sup>15</sup>.

$$\frac{\dot{q}'' H^2}{\dot{Q}_c} = 49 * Re^{-1/2} = 105 \left( \frac{\dot{Q}_c^{1/3} H^{2/3}}{\nu} \right)^{-1/2} \quad \text{Eqn 17}$$

His experiments verified the experiments of Yu and Faeth. The difference between the two correlations is that Alper's accounts for data obtained on turbulent jets which put the convective heat flux values about 50% greater [14].

These three correlations were then compared to what FDS calculated. The use of the HRR model of the seats was used to determine the  $Q_c$  for theoretical value.

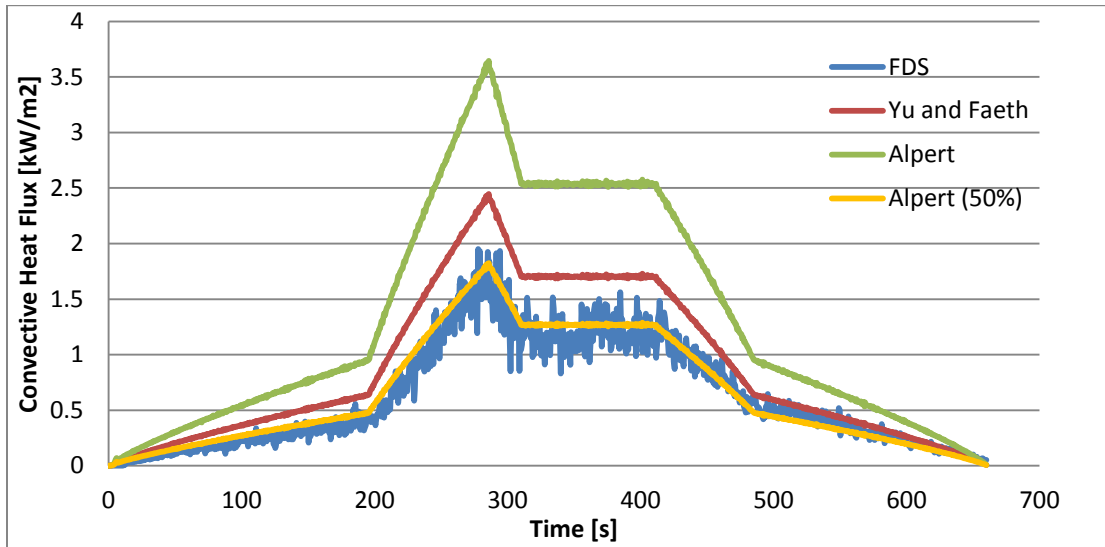
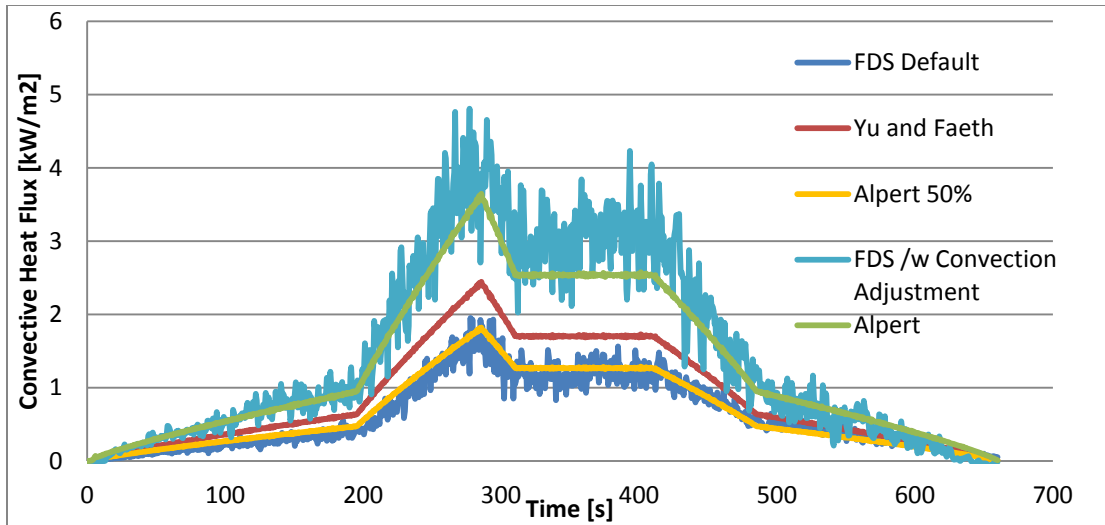


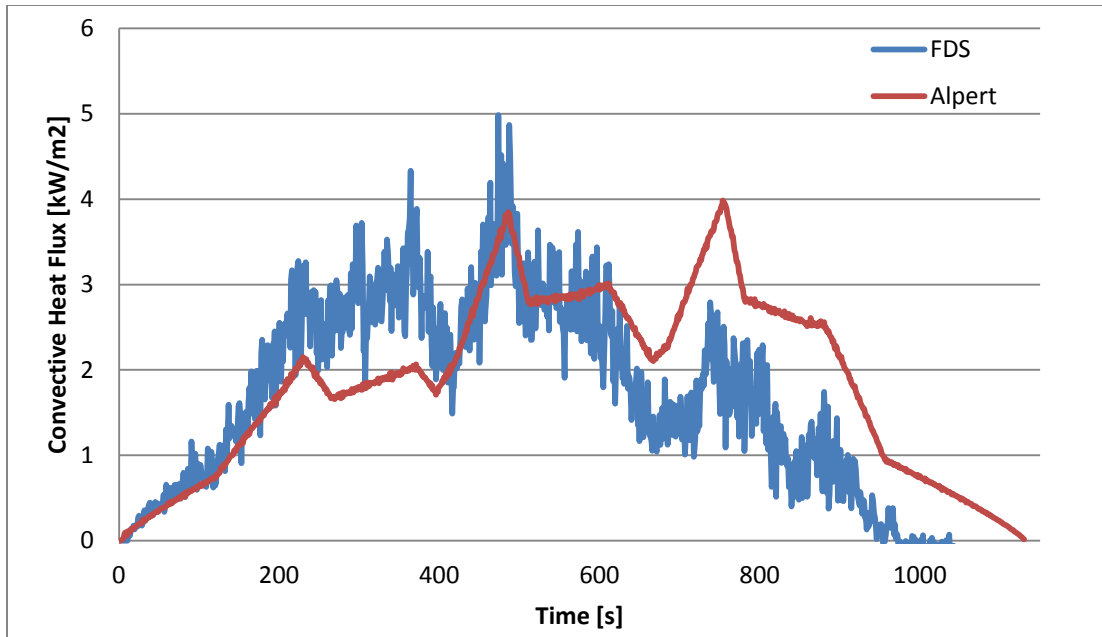
Figure 36: FDS vs theoretical values of convective heat flux at the ceiling.

Figure 36 shows that FDS is calculating the convective heat flux at the ceiling lower than what the theoretical value should be. It is similar to Alpert's correlation when accounting the 50% turbulent correction but is not near the value it could be. The FDS model's convective parameters were then adjusted so that the data is similar to Alpert's correlation which has the highest values.



**Figure 37: FDS vs theoretical values with convective correction.**

Using convective values of 6.08 for  $C_1$ , 5.24  $C_2$ , and 0.148  $C_F$ , the FDS model now matches close to Alpert's correlation. The new FDS values were four times greater than the default values. This new line represents the possible max value of convective heat flux that can occur at the surface of the upper deck. These corrections are then used in the model with the highest deck rise temperature which was the 5 seats with 2 rows backing up to each other.



**Figure 38: FDS with convection correction vs Alpert's for 5 by 5 seat orientation.**

Figure 38 shows the comparison of the highest theoretical correlation for convective heat flux to the FDS model of 10 chairs burning with the new convection coefficients. The model is fairly accurate to Alpert's with only fluctuating lower when the fire plume spreads away from the gauge. As the seats burn away, the initial center of the fire plume moves farther out where the other seats are burning. This causes the center of the plume to move away from centerline and thus causes the device to read lower values. The FDS values do follow the pattern of Alpert's correlation which is why it is assumed that the model is now representing these new maximum values.

The temperature within the space is a critical part when calculating heat transfer into boundary surfaces and is effected by the convective heat flux. The fire plume temperatures from FDS were compared with three temperature correlations to ensure that the temperature is being accurately calculated in the model and further validating the convective coefficients.

Alpert came up with a generalized theory to predict gas temperatures of a steady fire-driven plume for cases dealing with weak plumes [19]. The fires within the model are considered weak since the flame height is much less than the height of the space (using equation 14). His equation is widely used when trying to determine maximum gas temperature for hazard analysis calculations. Alpert's correlations are based on tests conducted using fuel arrays of wood and plastic pallets, empty cardboard boxes, plastic materials in cardboard boxes and liquid fuels ranging in size from 668 kW to 98 MW [14]. The correlations are broken into two parts applying to either the impingement or ceiling jet region of the fire plume. Data obtain in the model was taken from the impingement region since this is where the highest thermal values are within the plume. The maximum temperature within the impingement region, where  $r/H \leq 0.18$ , Alpert's correlation is:

$$T - T_{\infty} = 16.9 \frac{\dot{Q}^{2/3}}{H^{5/3}} \quad \text{Eqn 18}$$

where:

T = temperature, °C

H = ceiling height, m

Q = total heat release rate, kW

Heskestad developed nondimensional relations for maximum plume temperature based on alcohol pool fire tests [20].

$$\Delta T_0^* = \frac{\Delta T / T_{\infty}}{(\dot{Q}_0^*)^{2/3}} \quad \text{Eqn 19}$$

where:

T = temperature, °C

Q\* = nondimensional heat release rate.

Equation 19 represents the temperature within any region of the fire plume regardless of distance from the source. The value of  $\Delta T_0^*$  though is dependent on what region the

temperature is being taken. The value for  $\Delta T_0^*$  for the impingement regions is equal to 6.3 which is the maximum nondimensional value for temperature. Both Heskestad and Alpert's correlations have similar results and are typically recommended for prediction of steady ceiling jet flows beneath unobstructed ceilings like used in the 5A space model.

Morton developed an integral formulation for plume temperatures using the assumption of "top hat" profiles [21]. This top hat profile alters the three conservation equations of continuity, momentum, and buoyancy to where there is a uniform value across the radius of the plume. Values change over the elevation above the point source of the flame. Simplifying these equations to calculate plume temperature results in equation 18.

$$\Delta T_0 = 9.1 \left( \frac{T_\infty}{g c_p^2 \rho_\infty^2} \right)^{\frac{1}{3}} \dot{Q}_c^{\frac{2}{3}} (z - z_0)^{-\frac{5}{3}} \quad \text{Eqn 20}$$

where:

$T_0$  = centerline temperature, K

$T_\infty$  = ambient temperature, K

$g$  = gravity, 9.81 m/s<sup>2</sup>

$c_p$  = specific heat of air, 1.0 kJ/kg-K

$\rho$  = density of air, 1.2 kg/m<sup>3</sup>

$Q_c$  = convective heat release rate, kW

$z$  = elevation above point source, m

$z_0$  = virtual origin, m

All three correlations were used to verify the temperatures obtained in FDS. All three correlations come from extensive testing and are universally accepted in determining plume temperatures.

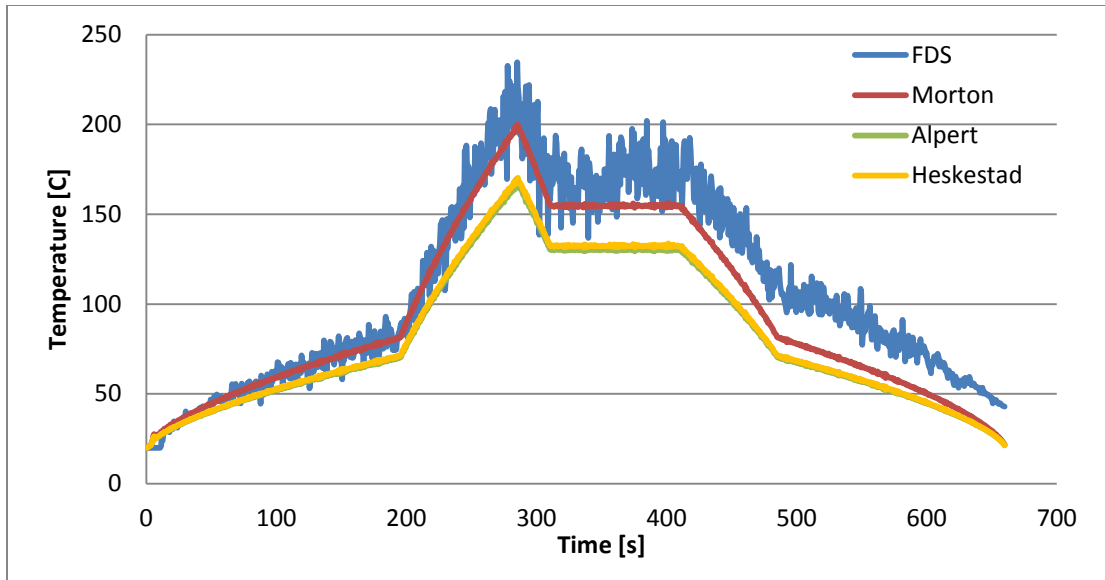


**Figure 39: Impingement region fire plume temperature.**

The values from FDS are conservative with the temperature values of the correlations by a few degrees after the growth phase of the fire. This means that the FDS results are closer to failure than what is to be expected. If the upper deck does not reach a critical temperature with all situations being at their highest values, it shows the deck will perform better in any situation. Comparing the FDS values to the three correlations for temperatures within the fire plume validates the accuracy of the temperature and convective models.

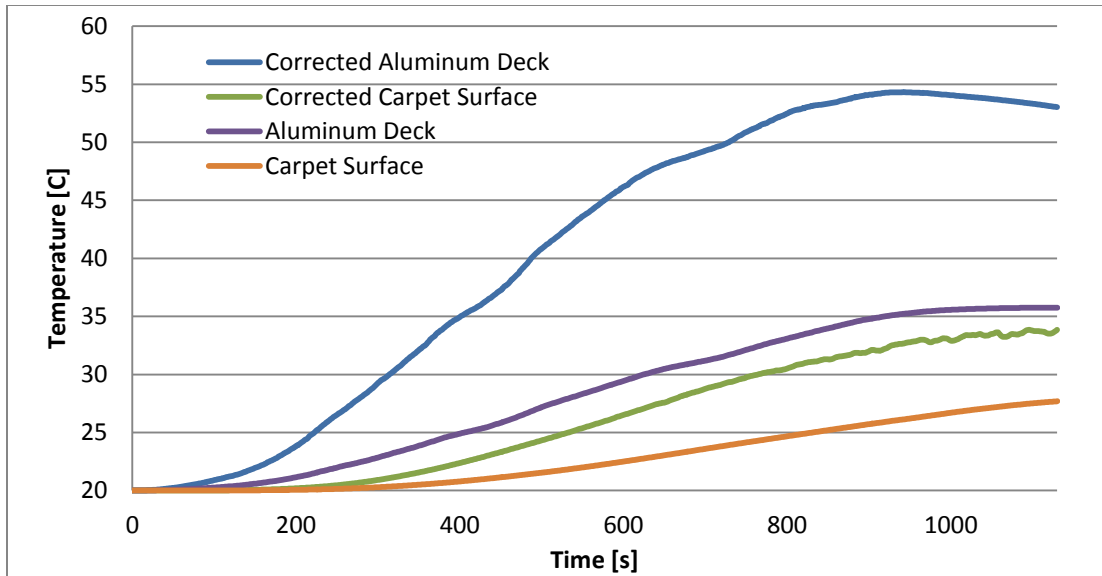


**Figure 40: Temperature comparison of the old and new convective coefficients.**

Using the validated convection coefficients the deck temperature increases by nearly double the previously calculated values. This is expected since there is twice the amount of convective heat flux on the surface of the deck. The top surface of the carpet is also added now to show what temperature passengers above would be subjected to during the fire. While the aluminum deck below reaches a max temperature around 55° C, the top surface of the carpet only reaches 35° C. Both values still do not reach any value that would cause structural integrity problems.

### Radiation

Thermal radiation transport is computed by default by FDS and no parameters are required to be changed to have this occur. However, there are certain aspects of the model that still can be adjusted to meet what is desired. Similar to convective coefficients, radiation transport has parameters that can be adjusted. Chapter 7 already discusses how the radiative fraction was obtained through full scale testing. This is the main parameter that is commonly changed since FDS can't reliably calculate

flame temperature and chemical composition in a large scale fire calculation because the flame sheet is not well-resolved [7].

The most common reason why a space flashes over is due to the re-radiation coming from the smoke boundary layer at the top of the space. The soot produced in a fire will re-radiate plume energy from the fire. The hotter this layer the more radiative heat flux is produced. Flashover will then occur once this reaches the ignition value for the materials within the space.

Heat flux data points were vertically oriented away from the seats to prevent obtaining readings of heat flux from the fire to measure the re-radiation heat flux from the smoke boundary. By isolating these gauges away from the fire source, they should only pick up any heat flux coming from the smoke layer, if any. The ten temperature data points were added at even intervals over a one meter span to determine the average smoke layer temperature. Extinction and absorption coefficient were also measured. All these values were used to calculate radiative heat flux.

Most of the heat transfer with radiation was accurately simulated by changing the radiative fraction when matching the heat flux gauges from the full scale testing to the small FDS model. As mentioned at the beginning of this section, radiation transport is a very complex part in modeling which takes into account many variables, some that are very difficult to determine. Thermal radiation from the hot upper smoke layer is a key factor in predicting compartment flashover. This factor can be readily calculated and is a good measure of the impact of a fire on a space. The amount of radiation emitted as compared to a blackbody is called emissivity. Emissivity is a fraction with values from 0 to 1. Typically no material has these two values and will usually reside

somewhere in the middle. The emissivity value for soot depends on the wavelengths over the theoretical smoke layer [11]:

$$\varepsilon = 1 - e^{-kS} \quad \text{Eqn 16}$$

where:

k = absorption coefficient of the smoke layer, 1/m

S = smoke layer height

Radiative heat flux can then be calculated using Planck's law which correlates

radiation to temperature:

$$\dot{q}_r'' = \varepsilon\sigma T^4 \quad \text{Eqn 17}$$

where:

$\sigma$  = Stefan-Boltzmann constant,  $5.87 \times 10^{-8} \text{ W/m}^2 \text{ K}^4$

T = temperature, K

The FDS model had added devices to obtain the temperature of the smoke layer over 1 m and absorption coefficient as seen in figure 41. These devices were located directly above where the heat flux was measured in order to have the most accurate temperature reading. Both the temperature and heat flux gauges were located away from the heat source in order to obtain mostly re-radiation heat flux values.

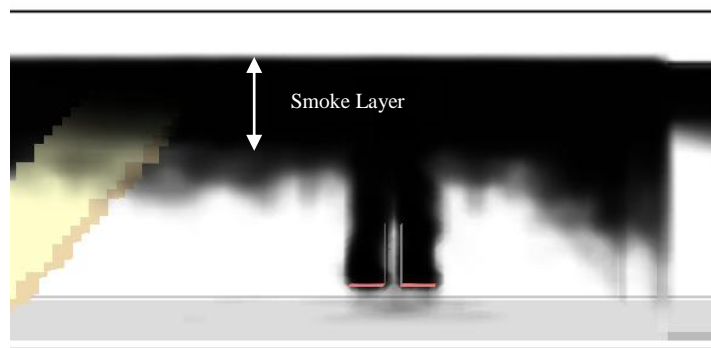


**Figure 41: Picture of the smoke layer used to determine temperature and absorption coefficient.**

The soot fraction of the seat materials was set to the highest yield found for these types of polycarbonates with a value of 0.23 [18].

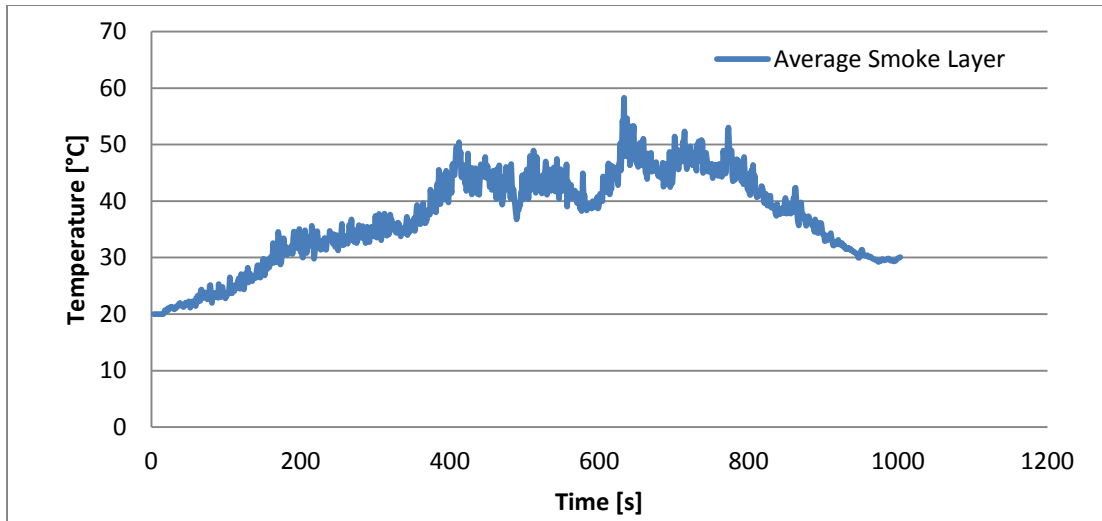


**Figure 42: Average smoke layer temperature over a 1 meter span.**

The average temperature is well below any value that could cause enough heat flux for flashover of the other seats within the space which would require a minimum of 9 kW/m<sup>2</sup>. Using equation 17 to determine the temperature required for the minimum ignition heat flux gives a value of 358° C. This is the average temperature of a smoke layer with a thickness of 1 m and a emissivity of 0.8 (maximum found in FDS testing). The highest temperature recorded measured for the smoke layer was only 100° C.

With lower temperatures in the smoke layer the total re-radiation value will be very minimal and not enough to cause flashover. The values from equations 16 and 17 were compared to the FDS calculates to ensure the simulation is portraying these values accurately.

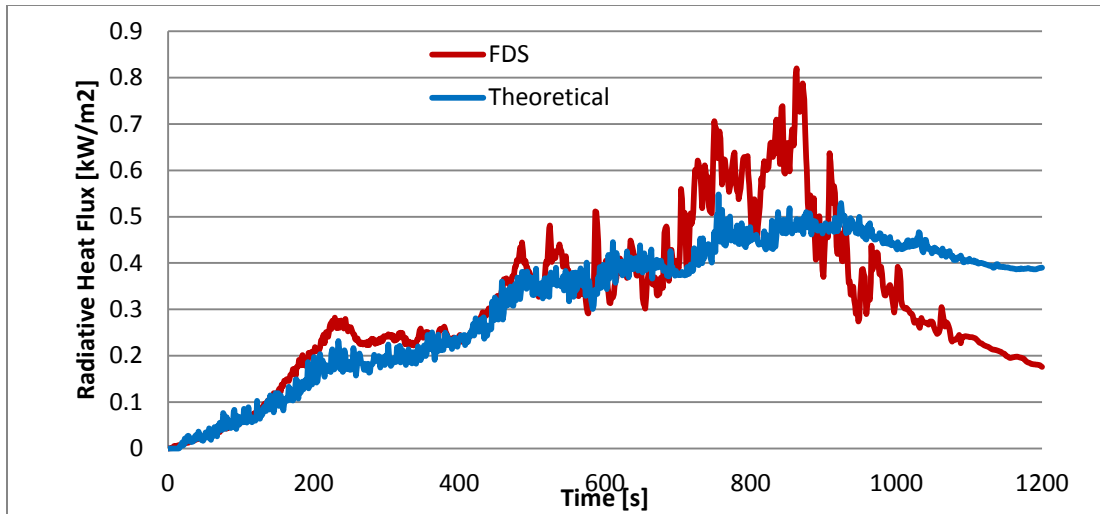
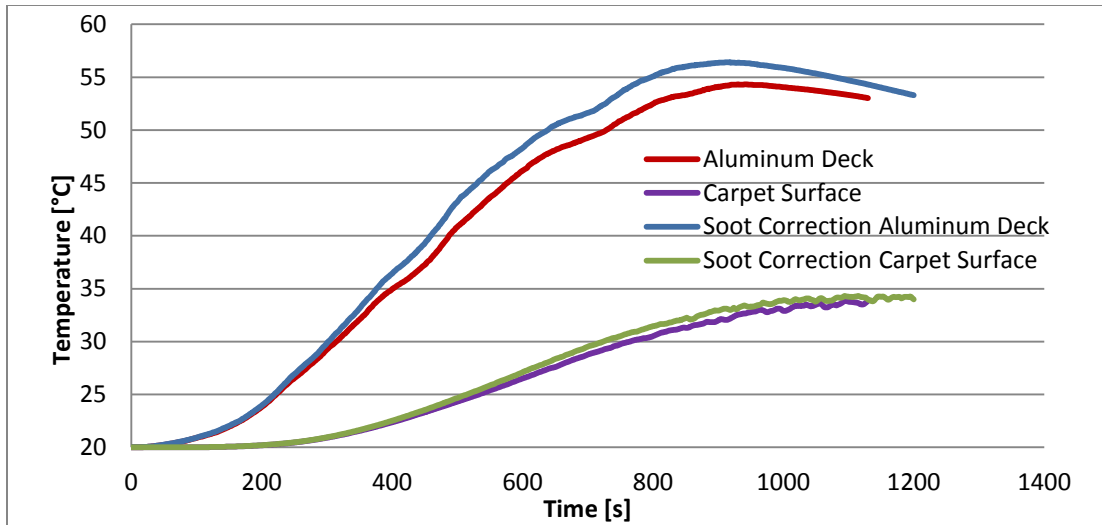


Figure 43: Smoke layer re-radiation value.

FDS calculates re-radiation from the smoke layer accurately to theoretical calculations. Some areas do fluctuate but that is considering FDS takes a dynamic approach to the smoke layer thickness instead of keeping it at a fixed value.

The addition of more soot, though, did cause the upper layer temperature to increase slightly but still well below any critical value. Figure 44 shows the final temperatures of the upper deck after adjusting the FDS model assuming maximum thermal values possible.



**Figure 44: Final upper deck temperatures with all corrections completed.**

### Conclusion

The evaluation of fire growth and structural integrity for type 5A spaces was analyzed using a variety of testing procedures. Testing accuracy was accomplished by incorporating full scale tests with CFD models, using the strengths of both types of methods.

Simple flammability tests and ignition tests ensured that combustible materials were accurately accounted for in the fuel load. Cone calorimetry was then used to determine ignition curves once it was determined that the only the foam chairs were the major contributor to the fire. The ignition curve for the chairs was then used to determine at what time a chair would ignite in the FDS simulations by correlating the average heat flux to its respective ignition time.

Full scale chair testing was then completed to determine the overall heat release rate.

This value was calculated using the mass loss rate obtained through testing and

multiplying it by the heat of combustion of the fabric and foam sample found in cone calorimetry testing. Once a heat release rate was calculated, a fitted linear line was used to simplify the noise of the curve to be added into the FDS code. Testing to calculate both the ignition curves and heat release curves with other means than FDS allows greater accuracy in the combustion model. This ensures that the simulation will accurately portray the combustion characteristics of the chairs.

A sensitivity analysis was done on the major input parameters controlling how FDS simulated the fire ensured that the model used to test the fire protection regulation for class 5A spaces is accurate.

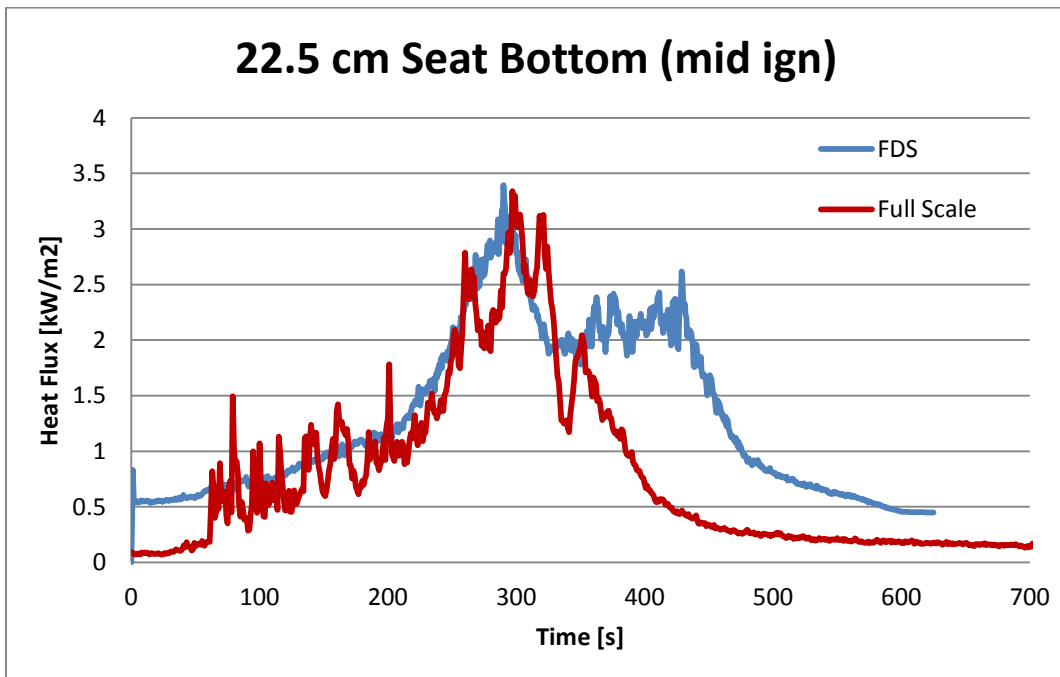
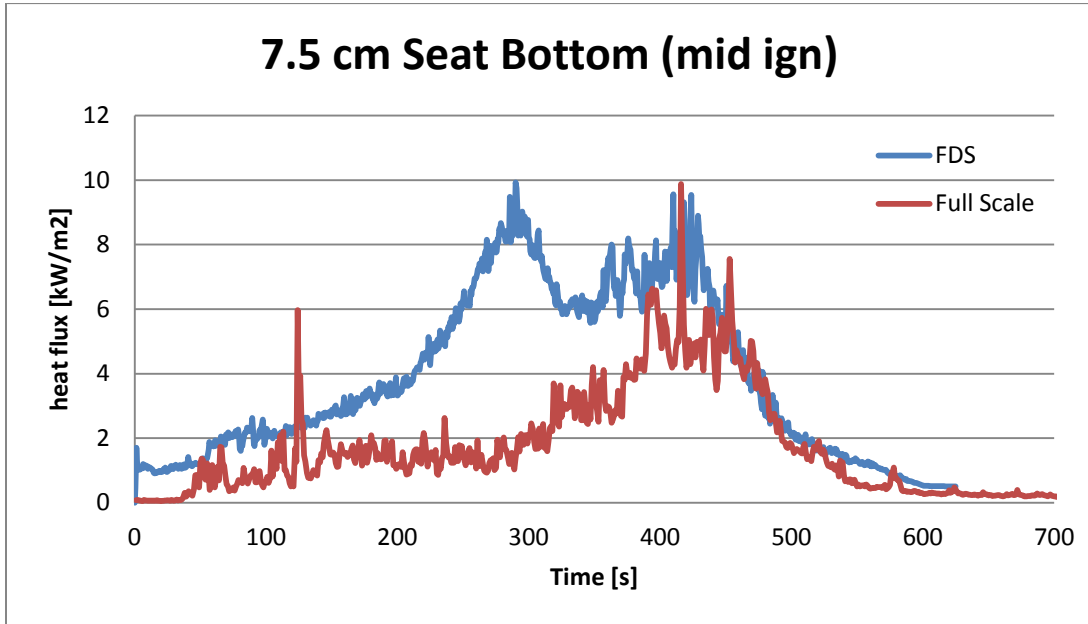
Radiative heat flux was corrected to match what was tested in full scale burning of the seats by modeling the burn lab in FDS. The value of 0.25 radiative fraction was determined to be the value at which the heat flux from full scale and FDS simulations were similar. The radiative fraction was then set to this value for all simulations.

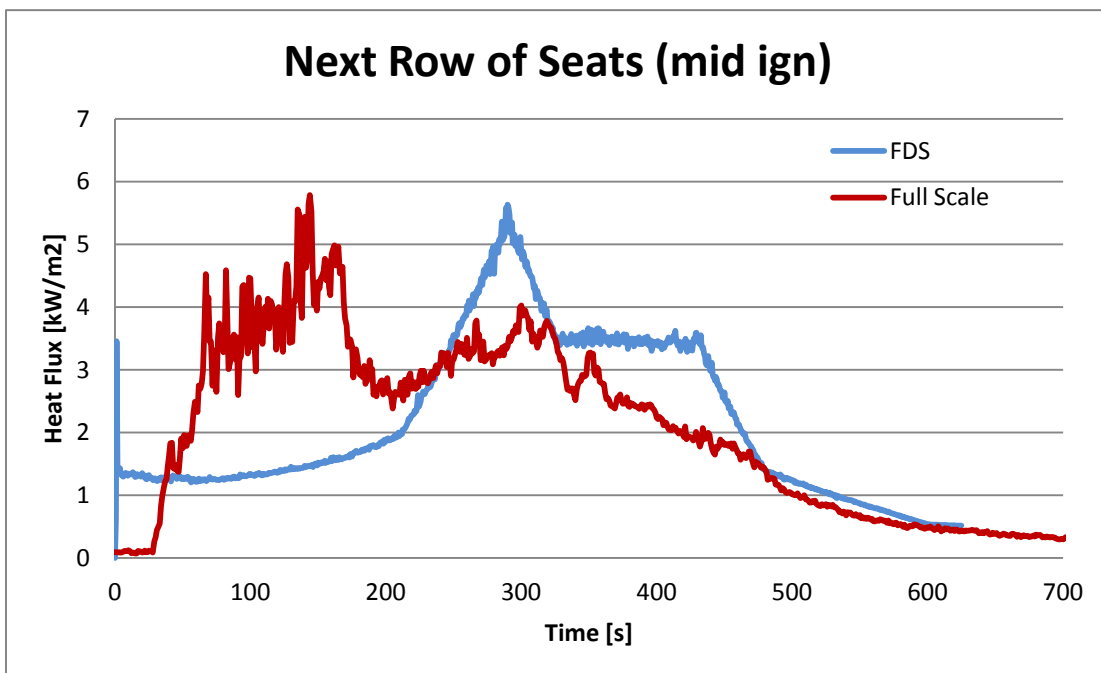
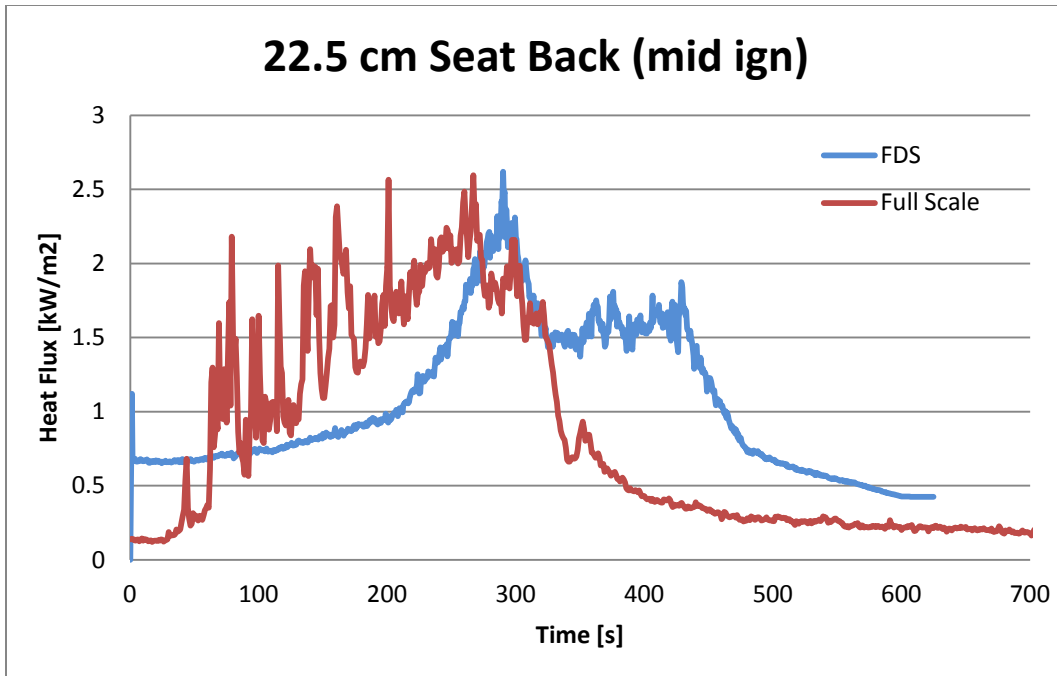
Varying the mesh size between ratios of 4 and 10 does affect the precision of the model but not to an extent to where previous values are considered inaccurate. Mesh size was an important aspect of the testing since all the simulations were completed on a standard desktop computer and averaged around 12 hours per simulation.

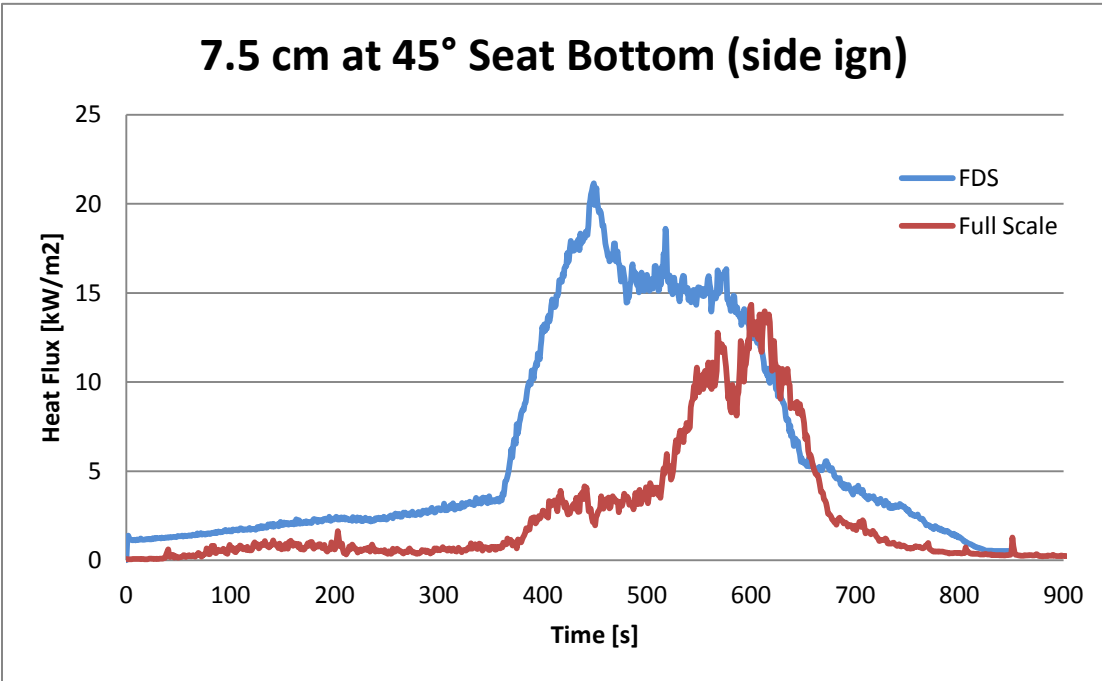
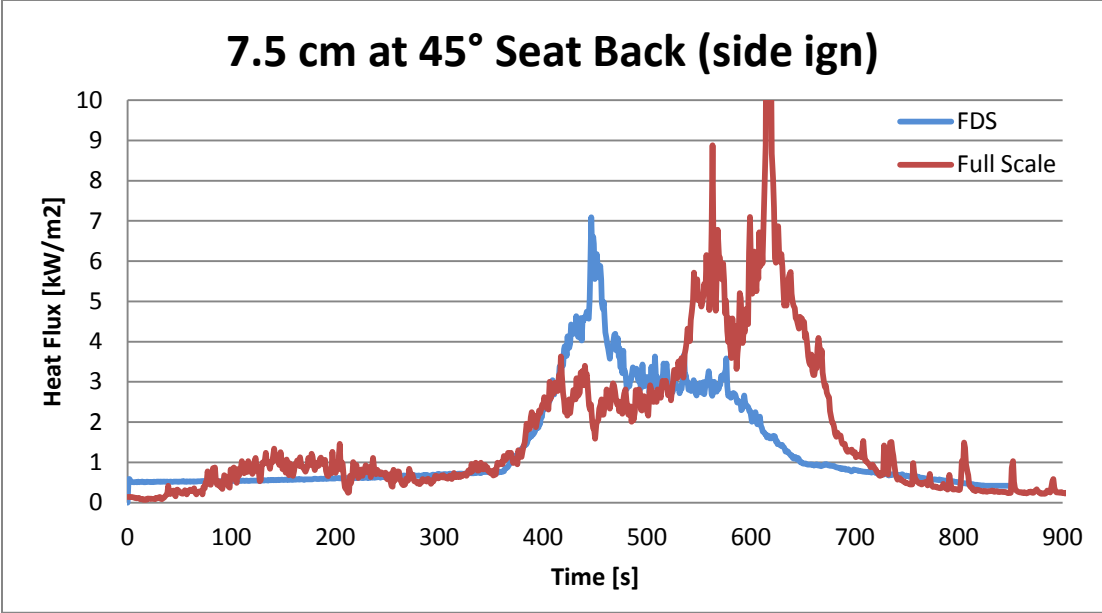
Convective heat transfer was considered the biggest thermal transport property in the simulations. The transfer of heat between the fire plume and upper layer was done majority by convection. Even when the convective coefficients were increased to four times the default values to match Alpert's correlation the upper deck temperature still only reached a value of 55 °C. This is still well below the critical value of 232 °C when aluminum starts to lose structural integrity.

With extensive testing through cone calorimetry, full scale burn tests, and FDS simulations, the regulation for class 5A spaces regulated by 46 CFR subchapter K and interpreted by NVIC 9-97 to only have maximum fire load of 5 kg/m<sup>2</sup> is acceptable. The extensive testing that occurred with a variety of methods show that the upper deck will not reach a critical temperature before the one hour stay time for passenger evacuations.

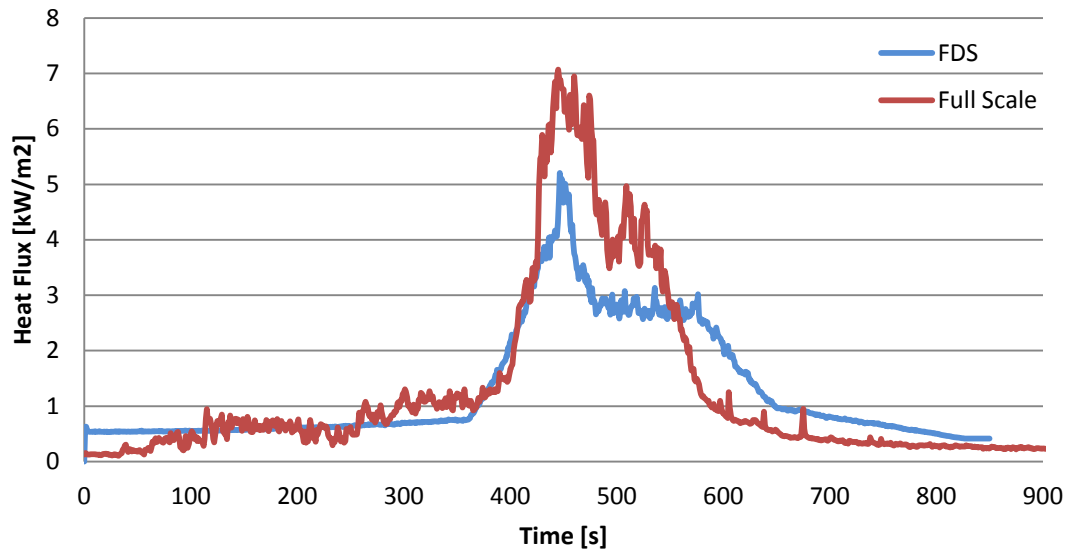
## Appendix A: Small Scale FDS vs. Full Scale Chair Testing



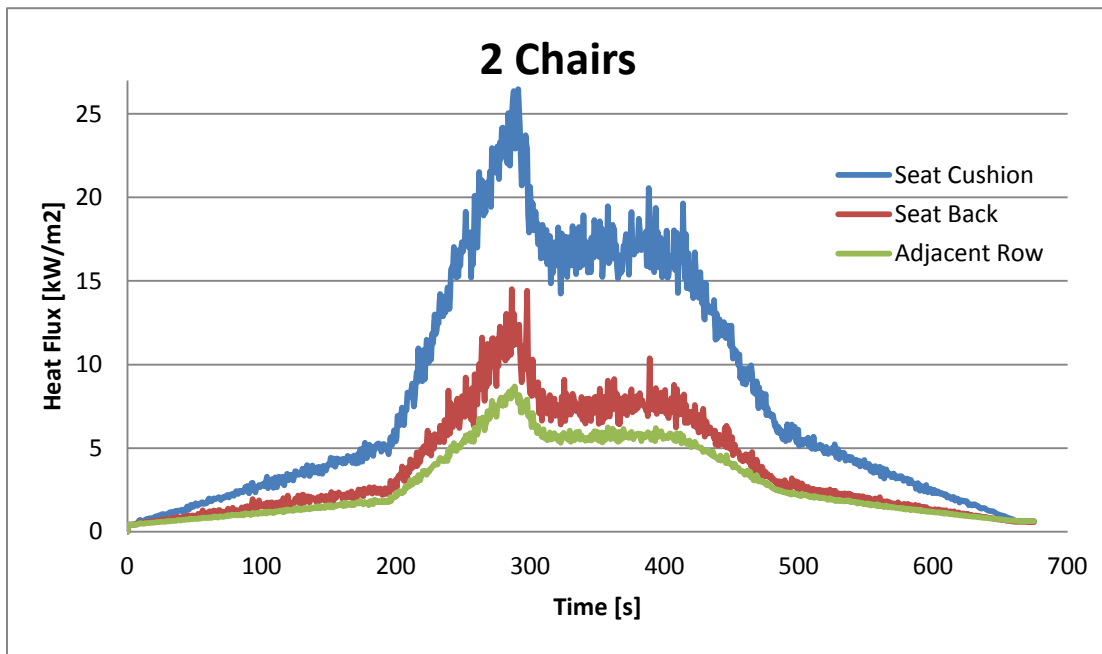
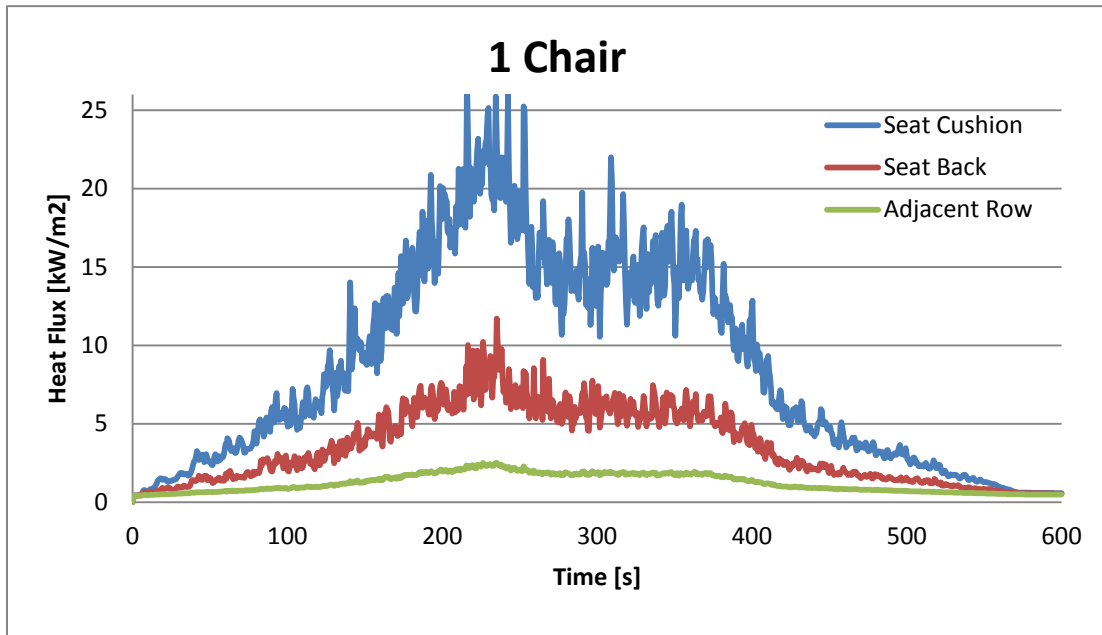


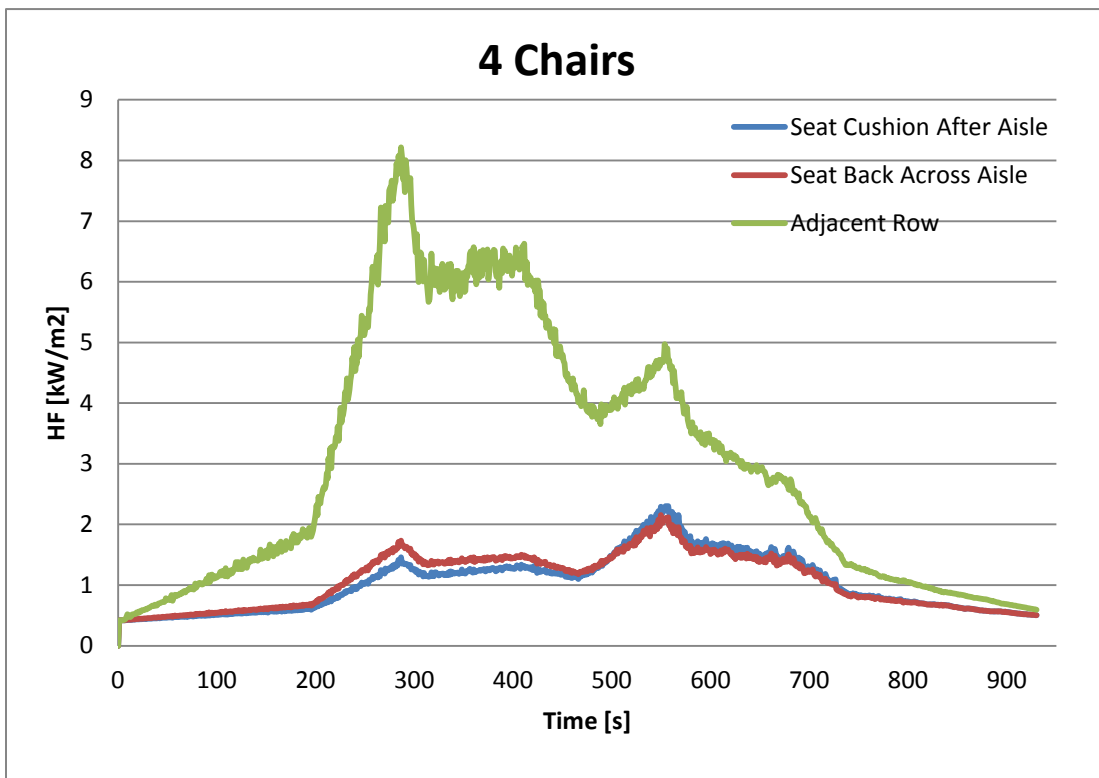
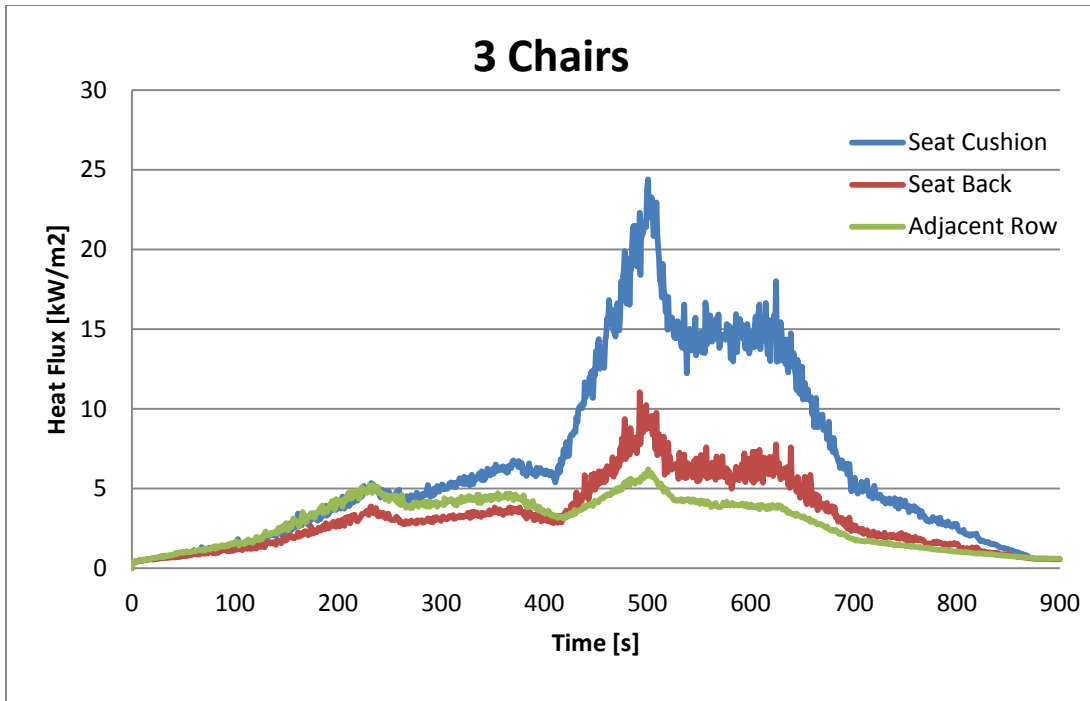


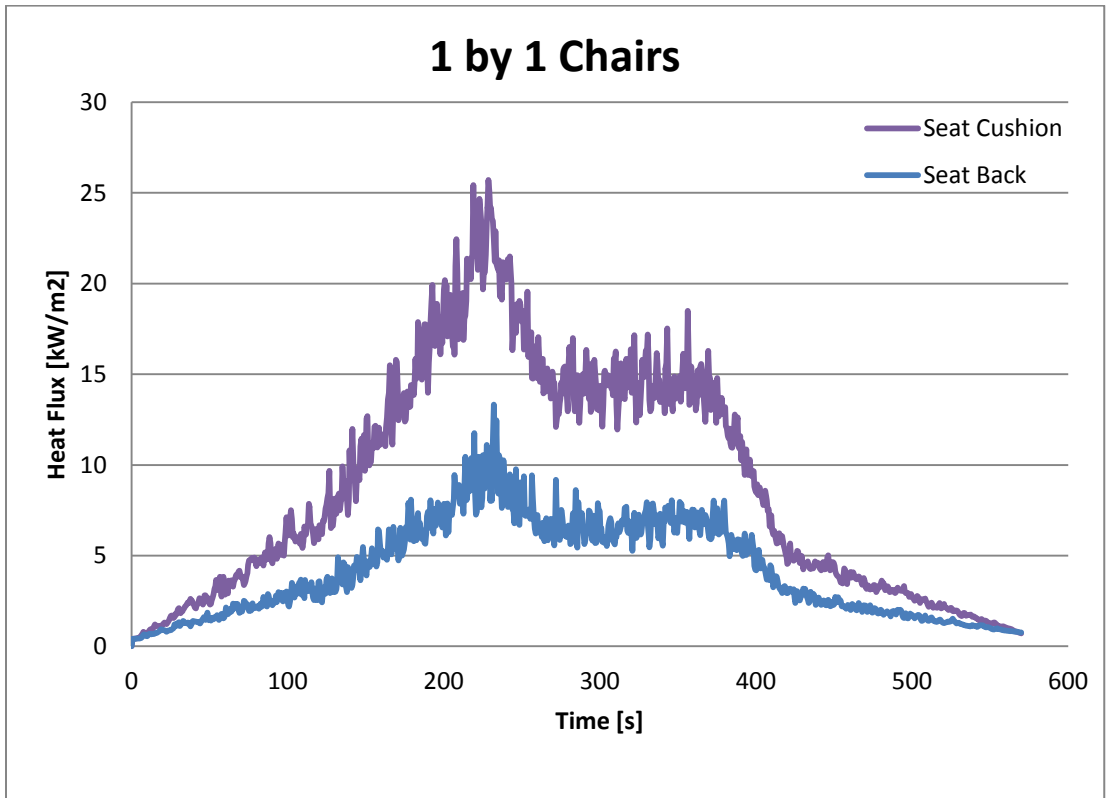
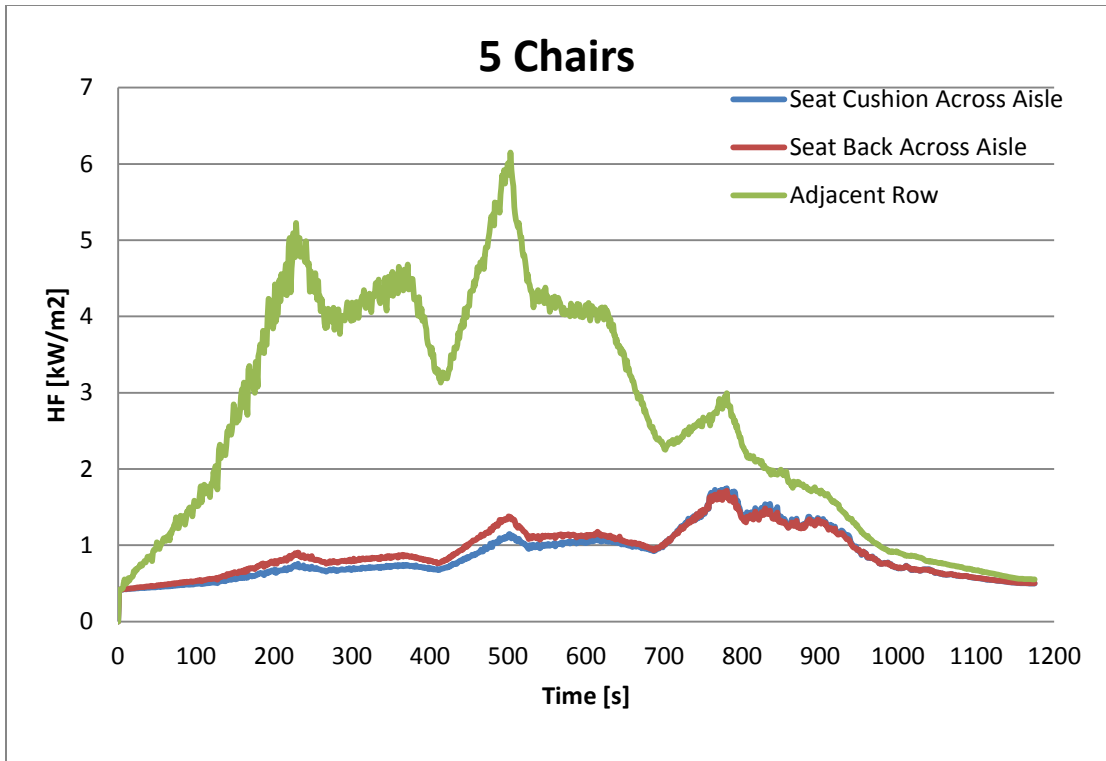
### 22.5 cm at 45° Seat Back (side ign)

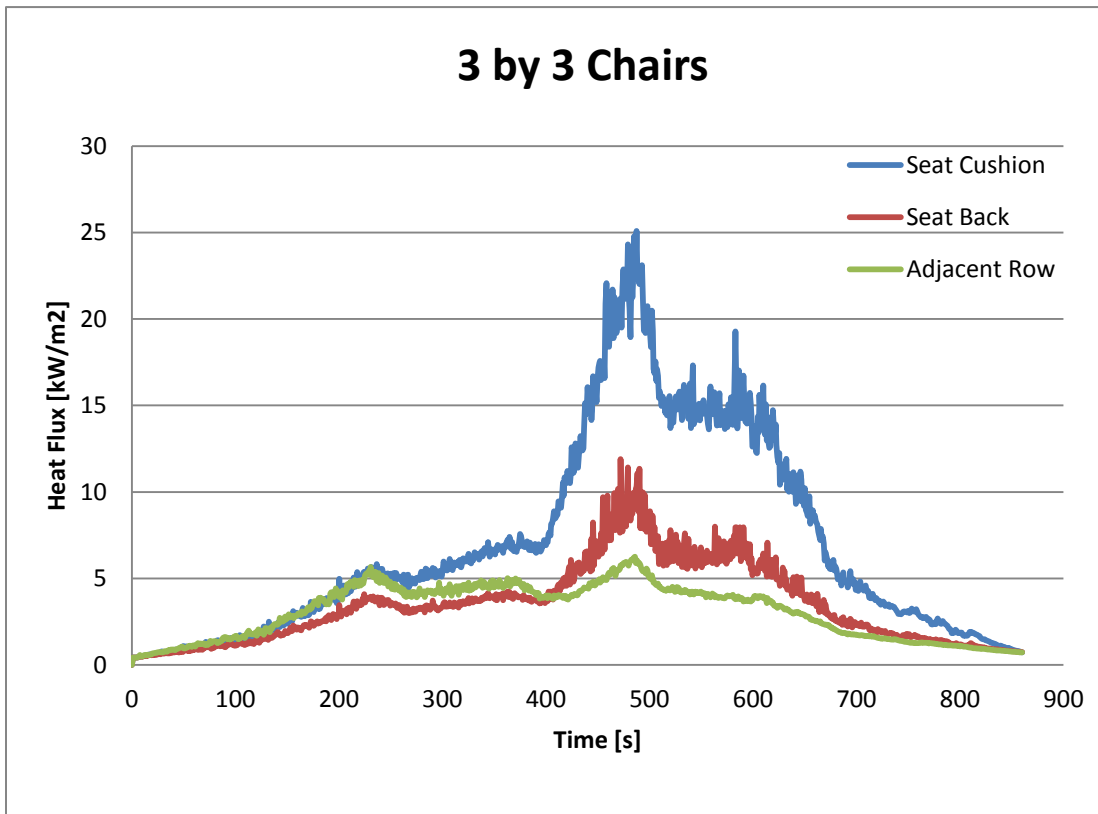
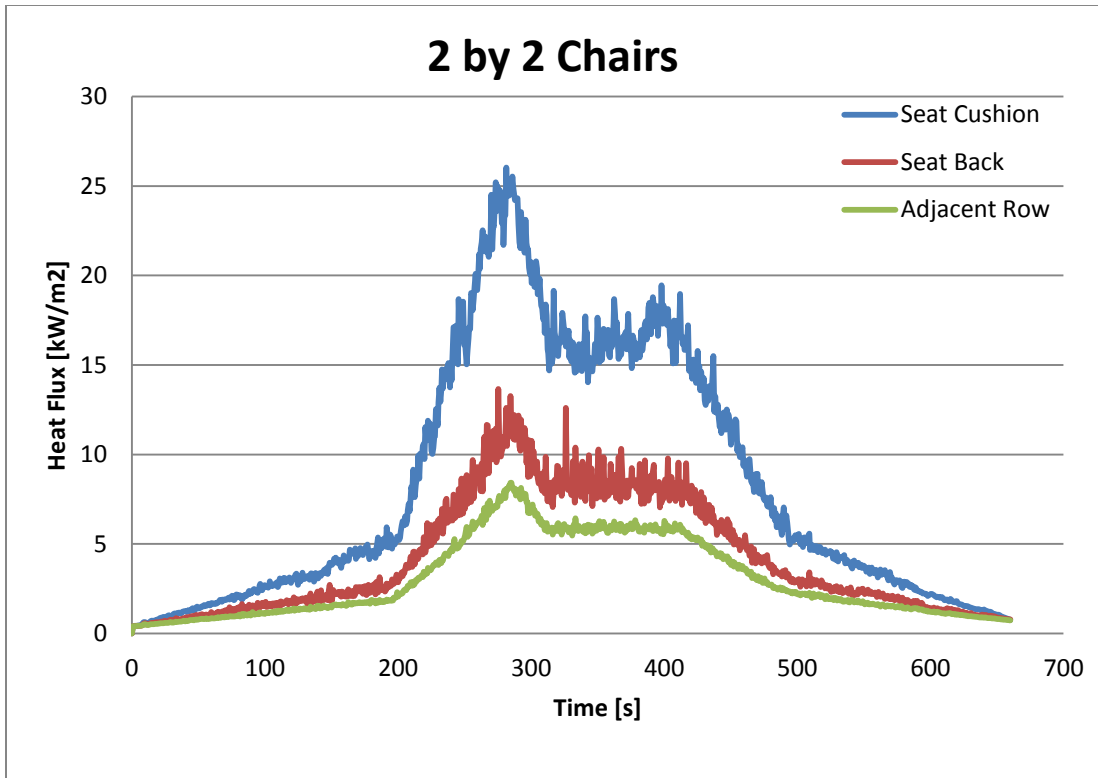


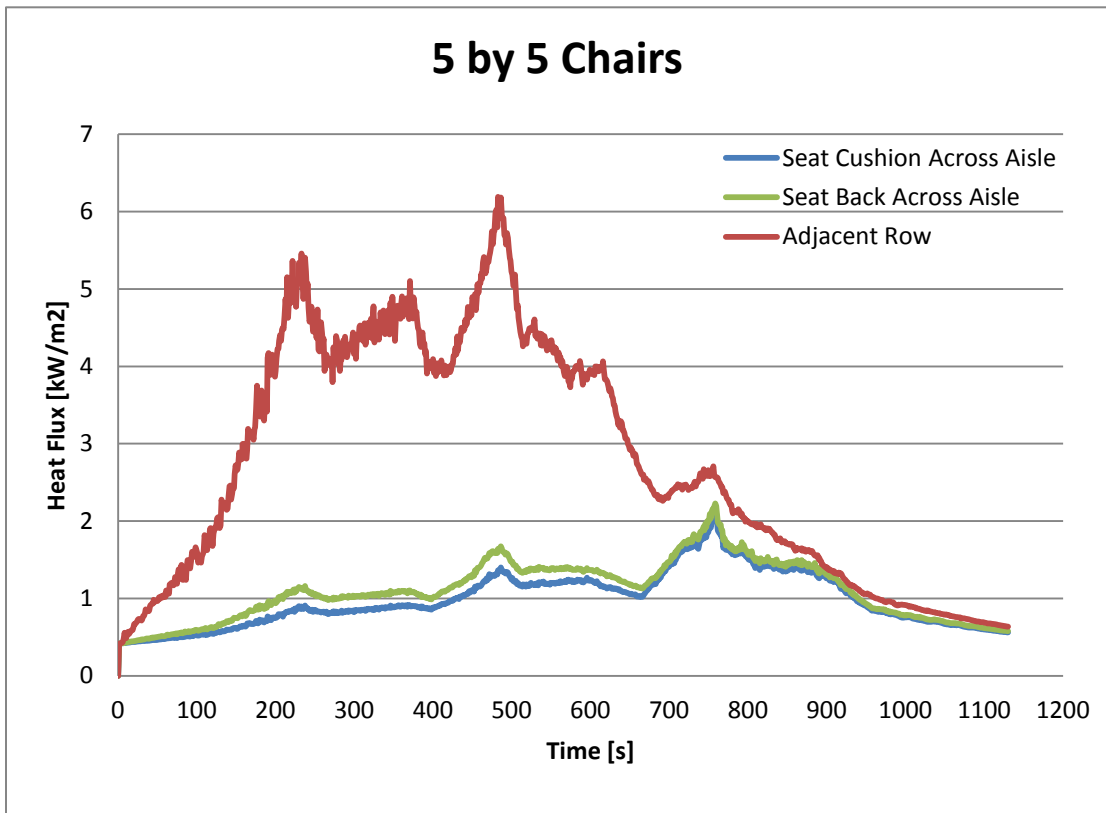
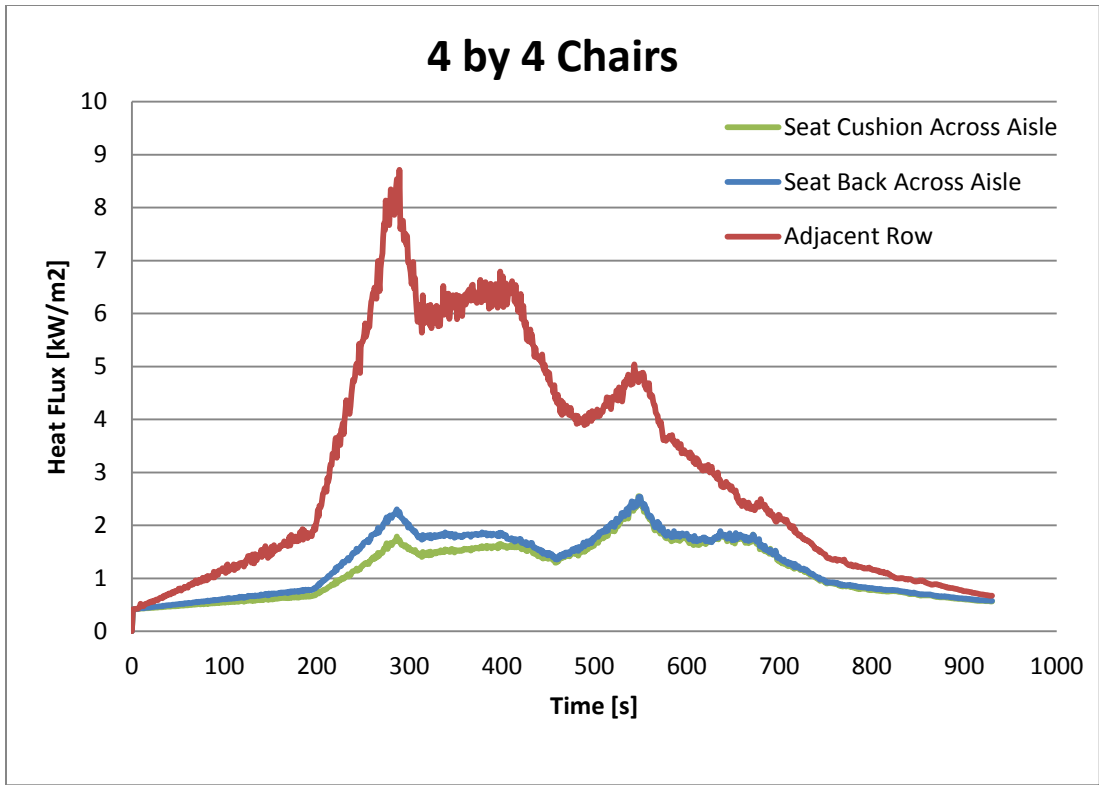
## Appendix B: FDS Full Scale Testing











## Bibliography

- [1] NVIC 9-97, Navigation and Vessel Inspections Circular Guide to Structural Fire Protection.
- [2] PFM 1-94, Policy File Memorandum on Structural Insulation Requirements for Low Fire Load Spaces on Certain Vessels.
- [3] Peatross, M.J., Beyler, C.L., Sprague, C.M., Dolph, B.L, "Low Fire Load Compartment Flashover Testing", Report No. CG-D-05-98, December 1997.
- [4] 46 CFR 114.400, Code of Federal Regulation for Small Passenger Vessels Carrying More Than 150 Passengers; Definition Section.
- [5] Janssens, M., "Calorimetry", *The SFPE Handbook of Fire Protection Engineering, Third Edition*, P. J. DiNenno editor, 2002.
- [6] Cox, G., Suresh, K., "Modeling Enclosure Fires Using CFD", *The SFPE Handbook of Fire Protection Engineering, Third Edition*, P. J. DiNenno editor, 2002.
- [7] National Institute of Standards and Technology, Gaithersburg, Maryland, USA, and VTT Technical Research Centre of Finland, Espoo, Finland. *Fire Dynamics Simulator, User Guide*, fifth edition, October 2010. NIST Special Publication 1019-5.
- [8] National Institute of Standards and Technology, Gaithersburg, Maryland, USA, and VTT Technical Research Centre of Finland, Espoo, Finland. *Fire Dynamics Simulator, Technical Reference Guide*, 5th edition, October 2007. NIST Special Publication 1018-5 (Four volume set).
- [9] Tan J., Shell Seraya Research Laboratory, Test Report SRN98-083, November 1998.
- [10] 46 CFR 116.423, Code of Federal regulations for Small Passenger Vessels Carrying more Than 150 Passengers; Construction and Arrangement, Fire Protection Furniture and Furnishings.
- [11] Quintiere, J.Q., *Fundamentals of Fire Phenomena*. John Wiley & Sons, LTD, September 2009.
- [12] Drysdale, D.D., "Thermochemistry", *The SFPE Handbook of Fire Protection Engineering, Third Edition*, P. J. DiNenno editor, 2002.

- [13] K. Hill, J. Dreisbach, F. Joglar, B. Najafi, K. McGrattan, R. Peacock, and A. Hamins. Verification and Validation of Selected Fire Models for Nuclear Power Plant Applications. NUREG 1824, United States Nuclear Regulatory Commission, Washington, DC, 2007.
- [14] Alpert, R.L, "Ceiling Jet Flows", *The SFPE Handbook of Fire Protection Engineering, Third Edition*, P. J. DiNenno editor, 2002.
- [15] Heskestad, G., *Combustion and Flame*, 83, p 293, 1991.
- [16] Alper, R.L, "Convective heat Transfer in the Impingement Region of a Buoyant Plume", *ASME J. of Heat Transfer*, 109, pg 120, 1987.
- [17] Yu, H.Z., and Faeth, G.M., *Fire and Materials*, 3, pg 140, 1979.
- [18] Tewarson, A. "Generation of Heat and Chemical Compounds in Fires". *The SFPE Handbook of Fire Protection Engineering, Third Edition*, P. J. DiNenno editor, 2002.
- [19] Alpert, R.L, *Fire Technology*, 8, pg 181, 1972.
- [20] Kung, H.C., Spaulding, R.D, and Stavrianidis, P., "Fire Induced Flow under a Sloped Ceiling", *Fire Safety Science, Proceedings of the Third International Symposium*, Elsevier Applied Science, New York, pg 271, 1991.
- [21] Morton, B.R., Taylor, G.I., and Turner, J.S., *Proc. Roy. Soc.*, A234, 1959.
- [22] Kodur, V.K.R, "Properties of Building Materials", *The SFPE Handbook of Fire Protection Engineering, Third Edition*, P. J. DiNenno editor, 2002.